2022

Characterizing the LIR Domain of ABIN1 and Identifying its Role as a Regulator of Mitophagy

Andrew Rhiner

CHARACTERIZING THE LIR DOMAIN OF ABIN1 AND IDENTIFYING ITS ROLE AS A REGULATOR OF MITOPHAGY

BY

ANDREW RHINER

A thesis submitted in partial fulfillment of the requirements for the

Master of Science

Major in Biological Sciences

South Dakota State University

2022

THESIS ACCEPTANCE PAGE

Andrew Rhiner

This thesis is approved as a creditable and independent investigation by a candidate for the master's degree and is acceptable for meeting the thesis requirements for this degree. Acceptance of this does not imply that the conclusions reached by the candidate are necessarily the conclusions of the major department.

Jaime Lopez
Advisor Date

Radhey Kaushik
Department Head Date

Nicole Lounsbery, PhD
Director, Graduate School Date

ACKNOWLEDGEMENTS

I would like to first thank my mentor Dr. Jaime Lopez for all his guidance on my journey. It is thanks to him that I have been able to learn all I have and get to begin my journey as a scientist. I am incredibly grateful for all the experience and wisdom he has granted me.

I would like to thank our collaborator Simin Rahigi for performing surface plasmon resonance.

I thank my laboratory colleagues who have worked alongside me and built a warm laboratory atmosphere, to include Quincee Simonson, Fredrick-Kumi Ansah, and Sylia Otchere. I would like to especially thank Katelyn Hurley, the only fellow member of the lab when I started and my mentor within the lab. I would not be the scientist I am without her help and am eternally grateful for her help.

I would next like to thank my committee members for their guidance with my work, Dr. Darci Fink, Dr. Adam Hoppe, Dr. Gergely Imre, and Dr. Robin Brown.

Finally, I would like to thank my family and friends back in Texas for their emotional support throughout the process. To my parents, Gary and Tracy, sister, Alexandria, and best friend, Sigrid, I am grateful to all your open ears and hearts through these trying times. To my brother Joshua, I would not be here if not for you. Losing you pushed me to do things we always talked about, I love you dearly.

CONTENTS

ABBREVIATIONS

4EBP-1: 4E binding protein-1

A20/TNFAIP3: TNF-α-induced protein 3

ABIN1/TNIP1: A20-binding inhibitor of NF-κB 1/TNFAIP3 Interacting Protein 1

ACC: Acetyl-CoA Carboxylase

AMPK: AMP-activated protein kinase

AP: Alkaline Phosphatase

ATG13: Autophagy-related protein 13

Baf. A1: Bafilomycin A1

Bort.: Bortezomib

CAMKK2: Calcium/Calmodulin Dependent Protein Kinase 2

CCCP: Carbonyl cyanide m-chlorophenyl hydrazone

cGAMP: Cyclic guanosine monophosphate (GMP)-adenosine monophosphate (AMP)

cGAS: cGAMP synthase (cGAS)

cIAP: cellular inhibitor of apoptosis protein-1

CYLD: Ubiquitin carboxyl-terminal hydrolase

DAMP: damage associated molecular pattern

DMEM: Dulbecco's Modified Eagle Medium

EBSS: Earle's Balance Salt Solution

ER: Endoplasmic Reticulum

FIP200: FAK family kinase-interacting protein of 200 kDa

FBS: Fetal Bovine Serum

IKK: IkappaB kinase

IRF3: Interferon regulatory factor 3

JNK: c-Jun N-terminal kinase

LC3: Microtubule-associated protein 1A/1B-light chain 3

LIR: LC3 interacting Region

LKB1: Liver Kinase B1

MEF: Mouse Embryonic Fibroblast

MLKL: mixed lineage kinase domain-like

mTOR: Mammalian Target of Rapamycin

myD88: Myeloid differentiation primary response 88

NDP52: Calcium-binding and coiled-coil domain-containing protein 2

NF-κB: Nuclear Factor Kappa B

p62/SQSTM1: Sequestosome-1

PAMP: pathogen associated molecular pattern

PBS: Phosphate Buffered Saline

PINK1: PTEN Induced Kinase 1

RIPK1: Receptor-interacting serine/threonine-protein kinase 1

RNF213: Ring Finger Protein 213

S6K-1: Ribosomal S6 Kinase-1

SDS: Sodium Dodecyl Sulfate

STING: Stimulator of Interferon Genes

TBK1: Tank Binding Kinase 1

TBS: Tris-Hydrochloric Acid Buffered Saline

TLR: Toll Like Receptor

TNF: Tumor Necrosis Factor

TNFR: TNF Receptor

TRAF: TNF Receptor Associated Factor

TRADD: Tumor necrosis factor receptor type 1-associated DEATH domain protein

Ub.: Ubiquitin

UBAN: Ubiquitin Binding Domain in ABIN proteins and NEMO

UBD: Ubiquitin Binding Domain

ULK1: Unc-51-like kinase 1

VPS: Vacuolar Protein-Sorting Protein

LIST OF FIGURES

ABSTRACT

CHARACTERIZING THE LIR DOMAIN OF ABIN1 AND IDENTIFYING ITS ROLE AS A REGULATOR OF MITOPHAGY

ANDREW RHINER

2022

A20 Inhibitor of NF-κB (ABIN1/TNIP1) is a known regulator of TNFα signaling induced cell death and inflammation. The regulatory activity has been attributed to ABIN1's recruitment of the ubiquitin editing enzyme TNF-α-induced protein 3 (TNFAIP3/A20) to Receptor-interacting serine/threonine-protein kinase 1 (RIPK1). The regulation of RIPK1 by ABIN1 and A20 relies on a third player, linear ubiquitin chain assembly complex (LUBAC), which is involved in the recruitment of ABIN1 to RIPK1. Loss of LUBAC or ABIN1 is embryonic lethal, but loss of A20 is not embryonic lethal. The embryonic lethality due to loss of ABIN1, paired with the lack of lethality with loss of A20, provides evidence that ABIN1 plays a role in cellular regulation beyond its role in recruiting A20 for RIPK1 regulation. We established that ABIN1 binds LC3 and is degraded in an autophagy-dependent manner. We also found that ABIN1 is a binding partner of mitochondria and plays a role in general housekeeping of mitochondria. ABIN1's regulation of mitophagy is an effect of its regulation of AMP-activated protein kinase (AMPK) phosphorylation, an upstream regulator of mitophagy. Loss of ABIN1 and its disruption of mitophagy appears to influence the release of mitochondrial DNA (mtDNA) from the mitochondria. The presence of mtDNA in the cytosol presents a potential explanation for Lupus in ABIN1 mutant patients.

Chapter 1: Introduction

Cells exist within an ever-changing environment where they must constantly adapt themselves at the molecular level to respond to changes. The core of maintaining cellular homeostasis is the balancing of anabolic and catabolic processes within the cell to adapt to changing environmental conditions and cell damaging events. Many of these processes are regulated by post translational modifications such as phosphorylation, ubiquitination, glycosylation, and lipidation[1-3]. One pathway responsible for regulating the balance of anabolic and catabolic activity is autophagy, a process that allows the cell to break down unwanted proteins and organelles and recycle them for further use. Macroautophagy, hereafter referred to as autophagy, involves the trafficking of large proteins, protein complexes, organelles, and membranes to double membrane vesicles, called autophagosomes, that will terminally fuse with lysosomes and degrade their contents.

Autophagy is a tightly regulated process that requires precise signals to begin. Initiation of autophagy is in large part controlled by the balancing of AMPK and Mammalian Target of Rapamycin (mTOR) signaling[4]. AMPK and mTOR are both responsible for the phosphorylation of Unc-51-like kinase 1 (ULK1)(Autophagy related protein 1(ATG1) in yeast) but their separate phosphorylation sites have opposing effects. AMPK phosphorylates ULK1 at Ser317 and Ser777, inducing its activation and therein promoting autophagy. mTOR phosphorylates Ser757, which prevents binding of AMPK and ULK1, in turn preventing the initiation of autophagy. These competing phosphorylation signals allow for the balancing autophagy activity based on nutrient availability.

Autophagosome formation

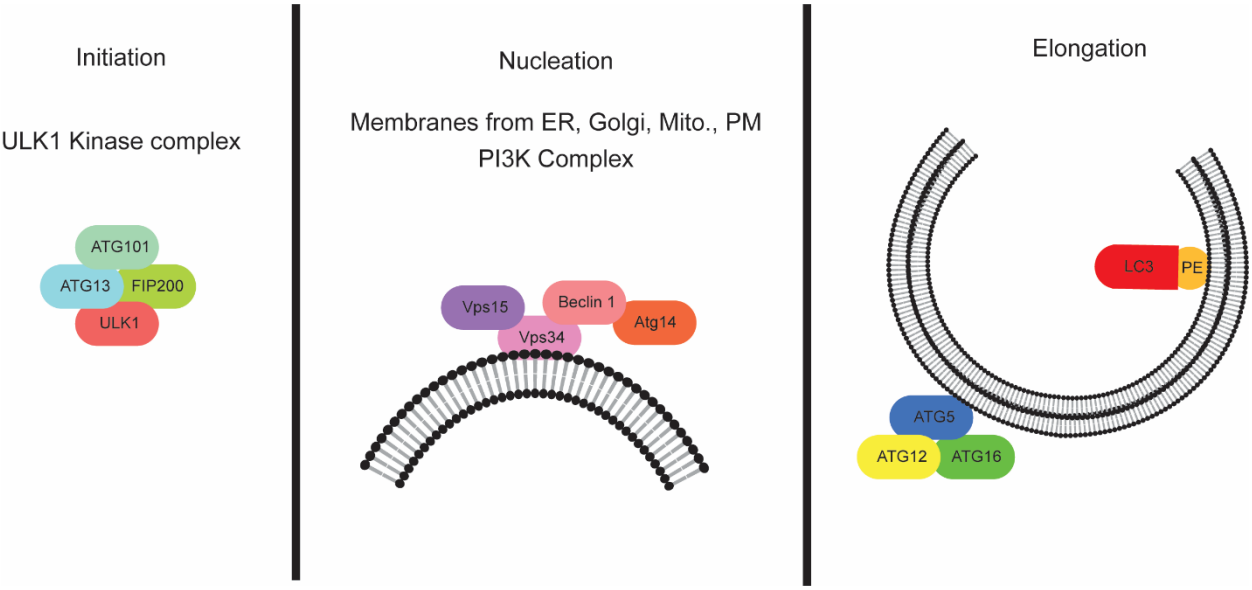

Figure 1.1 Schematic of autophagosome formation

Schematic of the three steps of autophagosome formation. Initiation begins with the phosphorylation of ULK1 and its subsequent phosphorylation of the members of its complex, ATG13, FIP200, and ATG101. Nucleation relies on the PI3K kinase Vps34 sequestering phospholipids from existing membranes. The third step, elongation, continues the nucleation and studs the exterior and interior of the forming phagophore with ATG proteins.

The formation of autophagosomes has three steps: initiation, nucleation, and elongation (Figure 1.1)[5]. Initiation begins with the activation of ULK1 by phosphorylation of Ser317 and Ser777, which only become available when mTOR is inhibited[6]. When nutrients are abundant and growth signaling is present mTOR is active and ULK1 is inhibited. Once nutrients become sparse mTOR becomes inactivated and allows AMPK to access ULK1 and phosphorylate it. ULK1 forms a complex with FAK

family kinase-interacting protein of 200 kDa (FIP200), ATG13 and ATG101. The ULK1 complex is responsible for the initiation of recruitment of ATG proteins for sequestering membranes[7].

The second step of autophagosome formation, nucleation, relies on Vacuolar Protein-Sorting Protein 34 (Vps34), a membrane trafficking protein and part of a class III phosphatidylinositol 3-kinase complex (PI3K) along with Vps15, Beclin 1 and ATG 14 (Figure 1.1)[8]. The PI3K complex acts to form membranes utilizing lipid bilayers of the endoplasmic reticulum (ER), Golgi, mitochondria, recycled vesicles and plasma membrane[9, 10]. From these sources the forming phagophore grows out and forms a double membrane a characteristic that is distinct to autophagosomes. Another key area of autophagosome formation is the contact points between mitochondria and ER, which often forms the autophagosomes that will ultimately be responsible for engulfing and consuming the mitochondria[11]. In the PI3K complex Vps34 is responsible for generating phosphatidylinositol, while Beclin 1 regulates the recruitment of cofactors. Beclin 1 has been shown to regulate the formation of varying autophagosomes based on which proteins it recruits into the complex[12].

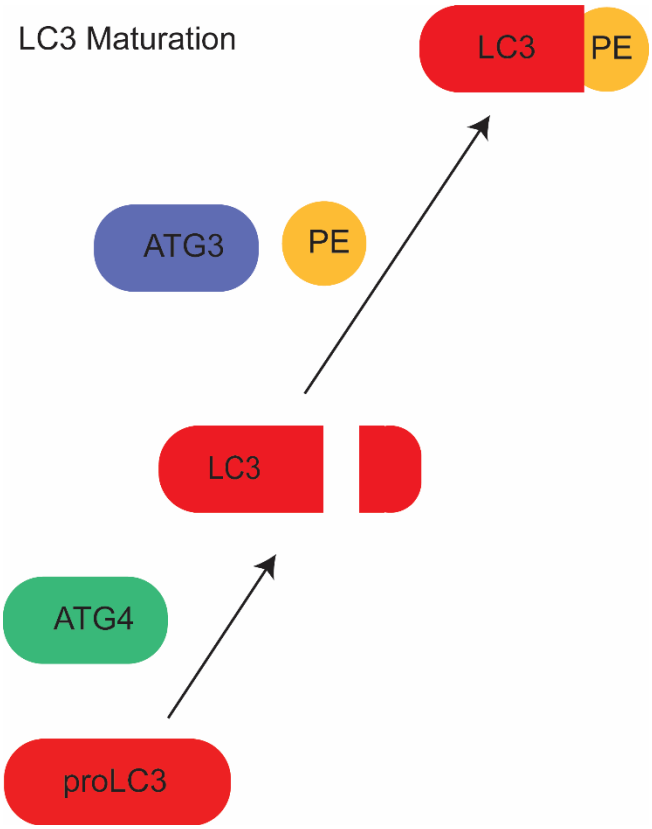

Figure 1.2 Schematic of LC3 maturation

Schematic of LC3 maturation. ProLC3 is cleaved by ATG4, LC3 is then lipidated by ATG3 which attaches a phosphatidylethanolamine. Lipidated LC3 is then studded into the interior of a phagophore.

The third step to autophagosome formation is elongation, which involves the simultaneous elongation and nucleation of the phagophore along with two ubiquitin-like protein conjugation systems (Figure 1.1). The first of these involves the formation of a complex with ATG5, ATG12, ATG16[13]. ATG5 is first covalently attached to ATG10 by ATG7, before being transferred to ATG12 followed by the attachment of ATG16 to ATG5 to form a mature complex that then forms heterodimers with other complexes. This complex is responsible for assisting in the development of the maturing autophagosome. Simultaneously, a second conjugation system is responsible for the generation of mature

LC3, which will eventually stud the interior of the autophagosome and regulate recruitment of substrates that need to be degraded (Figure 1.2)[14]. The ubiquitin-like system starts with proLC3 being cleaved by the cysteine protease ATG4. Cleaved LC3 is then lipidated by ATG7 and ATG3 to attach phosphatidylethanolamine (PE) which allows for the embedding of the LC3 into the inner membrane of the expanding autophagosome. Once the autophagosome has finished forming and is studded with LC3 it will either begin to engulf what is around it, if formed around the substrate it is intended to degrade, or split, from the membrane source and form an independent structure where it is then sequestered to the area of the cell it is needed.

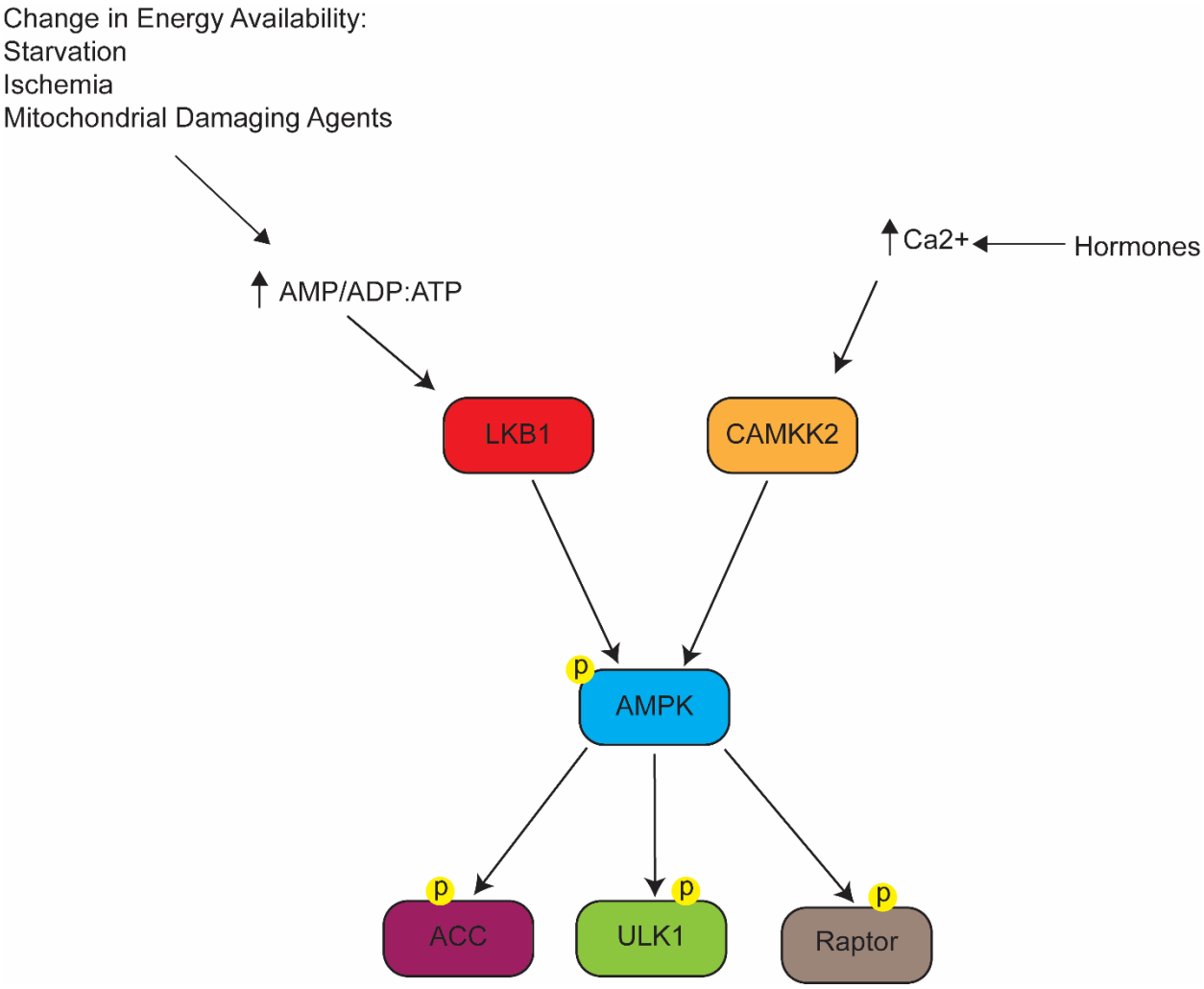

Figure 1.3 Schematic of AMPK pathway

AMPK pathway detects changes in nutrient availability and activates catabolic pathways in response. Decreases in metabolite availability, damage to mitochondria, ischemia or increases in Ca2+ levels cause LKB1 or CAMKK2 to phosphorylate AMPK at Thr 172. AMPK subsequently phosphorylates ACC, ULK1, and Raptor to inhibit anabolic pathways and initiate the autophagy-pathway.

AMPK activation

AMPK is the kinase responsible for phosphorylating ULK1 and triggering the autophagy pathway in which the autophagosome is formed. AMPK is a trimeric protein that acts as a nutrient sensor and becomes phosphorylated at Thr172 on AMPKα in

response to energy stress[15]. The activation of AMPK can be done by two different kinases depending on the source of stress (Figure 1.3). Liver Kinase B1 (LKB1) acts as a nutrient sensor by sensing changes in the ratio of AMP/ADP to ATP, and as the relative ratio of AMP increases the three parts of AMPK will colocalize and LKB1 will be recruited to them and phosphorylate AMPK[16]. The other kinase able to phosphorylate AMPK is Calcium/Calmodulin Dependent Protein Kinase 2 (CAMKK2), a calcium ion sensor that phosphorylates AMPK in response to fluxes in calcium levels, often triggered by hormones binding to membrane receptors. The phosphorylation will cause AMPK to become active and, in turn, phosphorylate three primary targets: ULK1—upregulating autophagy, ACC—inhibiting fatty acid and cholesterol synthesis, and Raptor —inhibiting mTOR[17]. AMPK upregulates a variety of catabolic pathways while simultaneously inhibiting anabolic pathways, making it a key regulator of cellular homeostasis.

mTOR pathway

In contrast to AMPK, mTOR works to inhibit catabolic processes and promote anabolic processes. mTOR phosphorylates ULK1 at Ser757, preventing its interaction with AMPK and as an effect of that downregulating autophagy. Simultaneously mTOR phosphorylates S6K-1 and 4EBP-1 to upregulate protein synthesis[18]. These two kinases work to balance the rate of autophagy within a cell and provide negative feedback loops for one another so that the upregulation of anabolic processes will downregulate catabolic processes and vice versa.

Structure of Autophagy Receptors

Autophagy is generally a selective process that is regulated by cargo receptors containing the LC3 interacting region (LIR) motif F/W/V-X-X-L/I/V. These cargo receptors act as scaffolding proteins to substrates that need to be degraded in autophagosomes[19]. These LIR containing proteins are referred to as autophagy receptors and are typically selective in their autophagy pathway, with many only acting in one of the selective autophagy pathways, and only a few being fairly promiscuous. The most well studied, and arguably the most promiscuous, is the autophagy receptor Sequestome 1 (p62/SQSTM1)[20]. p62 was first identified as a protein that shuttles protein aggregates to the autophagosomes to be degraded. Since then its role has grown and it has been found to act in almost all autophagy subtypes. While all autophagy receptors possess the capacity to bind LC3, another capability found among most selective autophagy receptors is the capacity to bind Lys-63 ubiquitin chains[21]. To date, approximately half of all known selective autophagy receptors have a ubiquitin binding region that binds Lys-63 ubiquitin chains, Met1 ubiquitin chains or both.

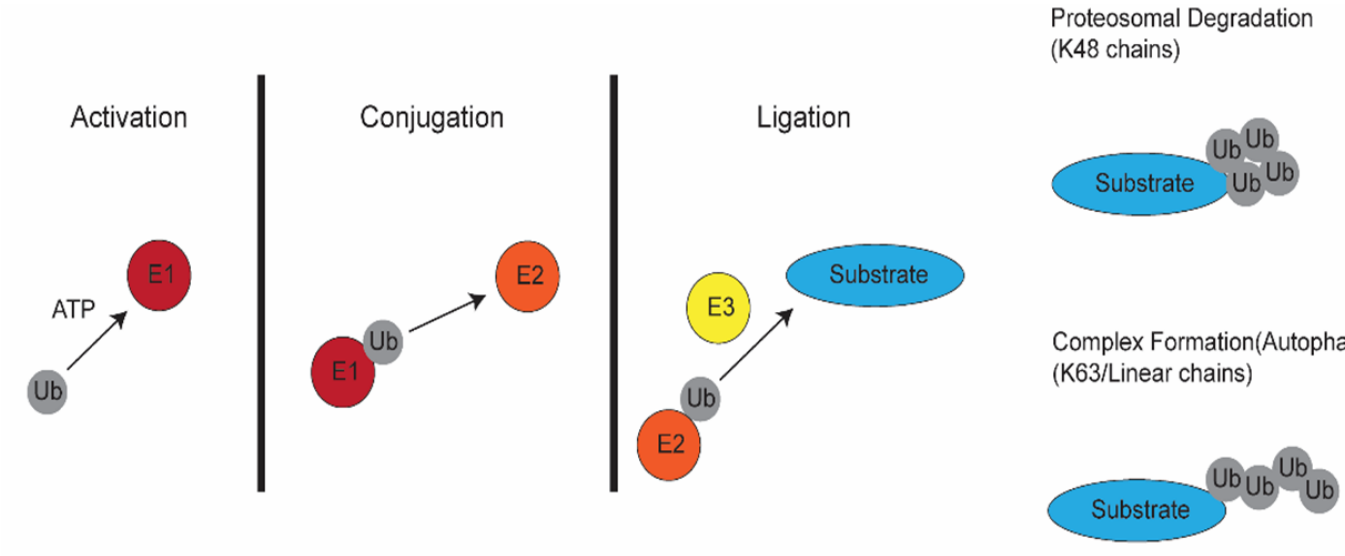

Figure 1.4 Schematic of ubiquitination

There are three steps to the conjugation of ubiquitin to a substrate. The first step is activation which is the attachment of ubiquitin to a ubiquitin activating enzyme, E1. The second step is conjugation where the E1 transfers the ubiquitin to a ubiquitin-conjugating enzyme, E2. The third step is ligation during which the E2 either transfers the ubiquitin to a ubiquitin ligase, E3, which will then attach the ubiquitin to a substrate or the E2 will attach the ubiquitin to the substrate in coordination with the E3. After the initial ubiquitin is attached to the substrate subsequent ubiquitin can attach to the already present ubiquitin to generate ubiquitin chains.

Ubiquitination of autophagy substrates

Post translational modifications are mechanisms cells utilize for a variety of purposes within a cell to active or inhibit, such as ULK1, as mentioned previously, alter structure, such as the lipidation of LC3 which allows it to become embedded in the autophagosome, and can also be used to determine the fate of a substrate. Ubiquitination, the attachment of an 8 kDa protein called ubiquitin, can mark substrates within the cell for degradation. Ubiquitination starts with the ATP dependent attachment of a ubiquitin to an E1 ubiquitin-activating enzyme, ubiquitin is then transferred to an E2 ubiquitin-conjugating enzyme and finally the ubiquitin is transferred to its target substrate via the coordination of an E2 and E3 ubiquitin ligase (Figure 1.4)[22]. E3 ubiquitin ligases have a great deal of specificity for what they will target as well as for the way in which they conjugate the ubiquitin chains. Ubiquitin can be conjugated as mono-ubiquitin, multi mono-ubiquitin, homotypic chains, or heterotypic chains[23]. The description of the chain is based on the area of linkage, namely which lysine on the previous ubiquitin the C-terminal glycine of the subsequent ubiquitin is attached to. The currently known ubiquitin chain types are Lys-11, Lys-27, Lys-29, Lys-33, Lys-48, and Lys-63 which each attach to a lysine and then Met-1, which attaches the C-terminal glycine of the subsequent ubiquitin to the N-terminal methionine of the previous ubiquitin. For the degradatory pathway, Lys-48 are associated with proteasomal degradation of the ubiquitinated substrate[24]. Lys-63

and Met-1 ubiquitin chains have both been found to function in the positive regulation of autophagy, but both ubiquitin chain types also possess roles in pathways outside of autophagy[25].

Selective Autophagy Subtypes

For selective autophagy there are a few specific classes of autophagy that involve the degradation of a particular organelle or pathogen. These include mitophagy (autophagy-dependent degradation of mitochondria), xenophagy (autophagy dependent degradation of intracellular bacteria), ERophagy (autophagy-dependent degradation of endoplasmic reticulum), and virophagy (autophagy-dependent degradation of viral capsids)[26-29]. Each of these selective autophagy subtypes have unique autophagy receptors associated with them, with some having overlapping promiscuous receptors. However, they all have the same outcome, degradation of cargo via lysosomes.

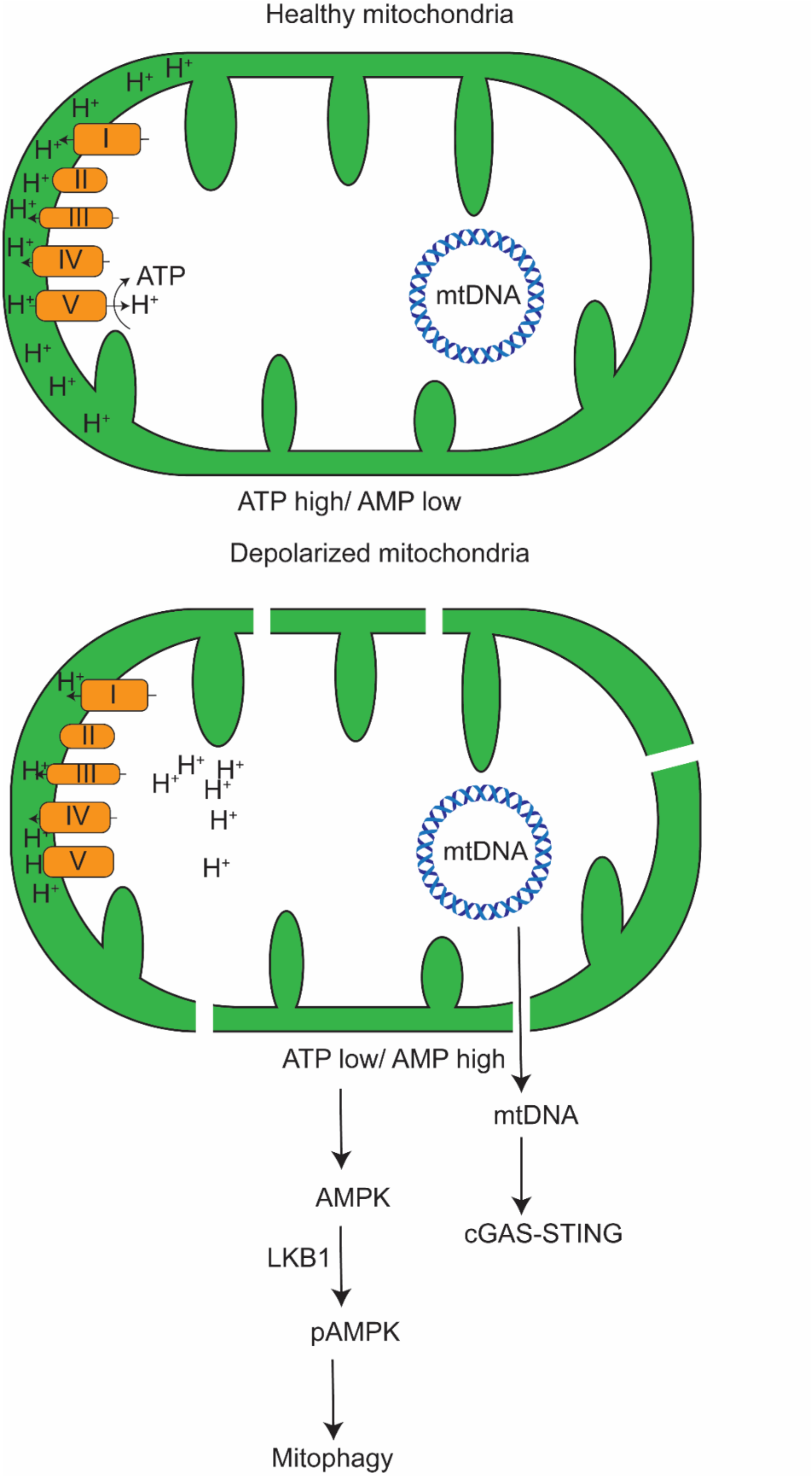
Healthy mitochondria
H+
I
II
III
IV
V
ATP
mtDNA
ATP high/ AMP low
Depolarized mitochondria
mtDNA
ATP low/ AMP high
mtDNA
AMPK
cGAS-STING
LKB1
pAMPK
Mitophagy

Figure 1.5 Schematic of mitophagy

When mitochondria become damaged and can no longer maintain a proton gradient, they become depolarized. Depolarization in turn causes the ratio of AMP:ATP to increase, since the mitochondria can now not generate sufficient ATP, inducing AMPK phosphorylation and the subsequent activation of the mitophagy pathway. Another biproduct of depolarizing mitochondria is increased permeability of the membranes which can allow mtDNA to escape from the mitochondria and activate the cGAS-STING pathway.

Mitophagy

The primary role of mitochondria in cells is generation of ATP, the primary energy source for cellular processes. Disruption to the production of ATP causes disruption in most metabolic processes of the cell, therefore maintenance of these organelles is vital. The production of energy exposes mitochondria to damaging molecules, specifically reactive oxygen species (a byproduct of energy production) that can induce damage to mitochondrial DNA as well as the proteins necessary for the generation of the ATP (Figure 1.5)[30, 31]. Mitochondria have developed intricate mechanisms to regulate their mitochondrial network, consisting of opposing forces of regular turnover and specific half-lives for each component coupled with mitochondrial biogenesis which adds new proteins and lipids to existing mitochondria. However, when it is necessary for entire mitochondria to be recycled due to damage or a decreased need for energy cells utilized the selective autophagy pathway, mitophagy.

Because of how vital mitophagy is, cells have developed a level of redundancy so if one set of proteins, such as mitophagy receptors, fails others can take over and still accomplish turnover of mitochondria. One of the most widely studied molecular pathways in mitophagy is the PTEN Induced Kinase 1 (PINK1)/Parkin pathway[32, 33]. When mitochondria are healthy, PINK1 has no place to bind on the outer membrane of the

mitochondria and is thus quickly degraded by the proteasome upon being shuttled out of the mitochondria. Upon mitochondrial damage when translocase of the outer membrane (TOM) proteins become damaged PINK1 can bind to the outside of mitochondria and becomes stabilized. Stabilization on the exterior of the mitochondria allows PINK1 to phosphorylate Parkin, an E3 ubiquitin ligase located on the exterior of the mitochondria, activating it and causing Parking to ubiquitinate substrates on the exterior of the mitochondria. The generation of Lys-63 chains signals to the cell to begin recruiting autophagy associated proteins to the mitochondria and subsequently induces mitophagy. When PINK1 or Parkin become disrupted the recruitment of mitophagy associated proteins becomes disrupted and cells struggle to maintain normal mitochondrial levels and in turn regulate their AMP:ATP levels. Interestingly, loss of a single mitophagy receptor is not detrimental to cells; it is only detrimental when two or more mitophagy receptors are lost that a significant difference in cells' ability to regulate mitochondrial levels occurs[26].

Xenophagy

Xenophagy is another selective autophagy receptor mediated form of degradation, but instead of degrading a cellular component it is responsible for the degradation of intracellular bacteria.[34] The current understanding is that when bacteria invade a cell, the cell marks them for degradation by the autophagosome. One of the ways xenophagy is understood to occur is by recruiting E3 ubiquitin ligases to the exterior of the cells, which will then generate ubiquitin chains on the LPS for autophagy receptors to bind.[35]. Ring Finger Protein 213 (RNF213) has been identified as the E3 ubiquitin ligase responsible for the initiation of the ubiquitination of the pathogenic bacteria *Salmonella* and *Toxoplasma gondii*[35]. *Salmonella* has been the most widely studied of the invasive pathogens due to

its ease of study. Analysis of *Salmonella* after the bacteria has invaded the cell revealed *Salmonella* gets Lys-63 and Met-1 ubiquitinated, which in turns drives it towards autophagosomal degradation[36]. It was originally thought that LUBAC, the only E3 ubiquitin ligase capable of generating Met-1 ubiquitin chains, was being directly recruited to the exterior of the pathogen. Recent work, however, has shown that the recruitment of LUBAC relies on the initial activity of RNF213, indicating that the cascade of ubiquitination on the exterior of invasive bacteria is dependent entirely on RNF213[37]. Another key player in xenophagy is the V-ATPase-Atg16L1 relationship[38]. Upon infection, *Salmonella* has been shown to become bound with V-ATPase, a proton pump that induces acidification of the pathogen. V-ATPase is essential for the recruitment of ATG16L1 to the bacteria, which then causes formation of the autophagosome around the pathogen.

Overlap between Mitophagy and Xenophagy

While mitophagy and xenophagy are two distinct processes and pathways, among the selective autophagy receptor subtypes they possess an interesting amount of overlap. Both rely on the activity of TBK1 to phosphorylate some of their autophagy receptors to increase binding activity, namely Optineurin (OPTN) in mitophagy and Calcium-binding and coiled-coil domain-containing protein 2 (NDP52) in xenophagy[39]. Beyond this, they have very similar pathways through which they act, as both rely on ubiquitination of the substrate, binding of autophagy receptors to the ubiquitin and subsequent shuttling of these autophagy receptors into the autophagosome. The overlaps between the selective autophagy of bacteria and mitochondria suggests that these pathways may evolved simultaneously, and that the specificity of the autophagy receptors is what sets them apart.

cGAS-STING

The cGAMP synthase (cGAS)- Stimulator of Interferon Genes (STING) pathway is an innate immune response that is activated upon sensing the presence of double stranded DNA (dsDNA)[40]. The sources of dsDNA can vary, but the most canonical activation is the infection of dsDNA viruses[41]. Upon dsDNA entering the cytosol, it activates the pathogen associated molecular pattern (PAMP) cGAS, which, in turn, activates the second messenger Cyclic guanosine monophosphate-adenosine monophosphate (cGAMP). STING then binds to cGAMP, which causes the complex to be transferred from the ER to the Golgi. The translocation and activation of cGAMP causes the downstream activation of Tank Binding Kinase 1 (TBK1), Interferon Regulatory Factor 3 (IRF3), and inflammatory cytokine production. The cGAS-STING pathway besides responding to viral dsDNA, will also recognize nuclear DNA, mtDNA, and bacterial DNA when present in the cytosol[42]. When mitophagy or xenophagy become disrupted, there is a causal opportunity for STING activation.

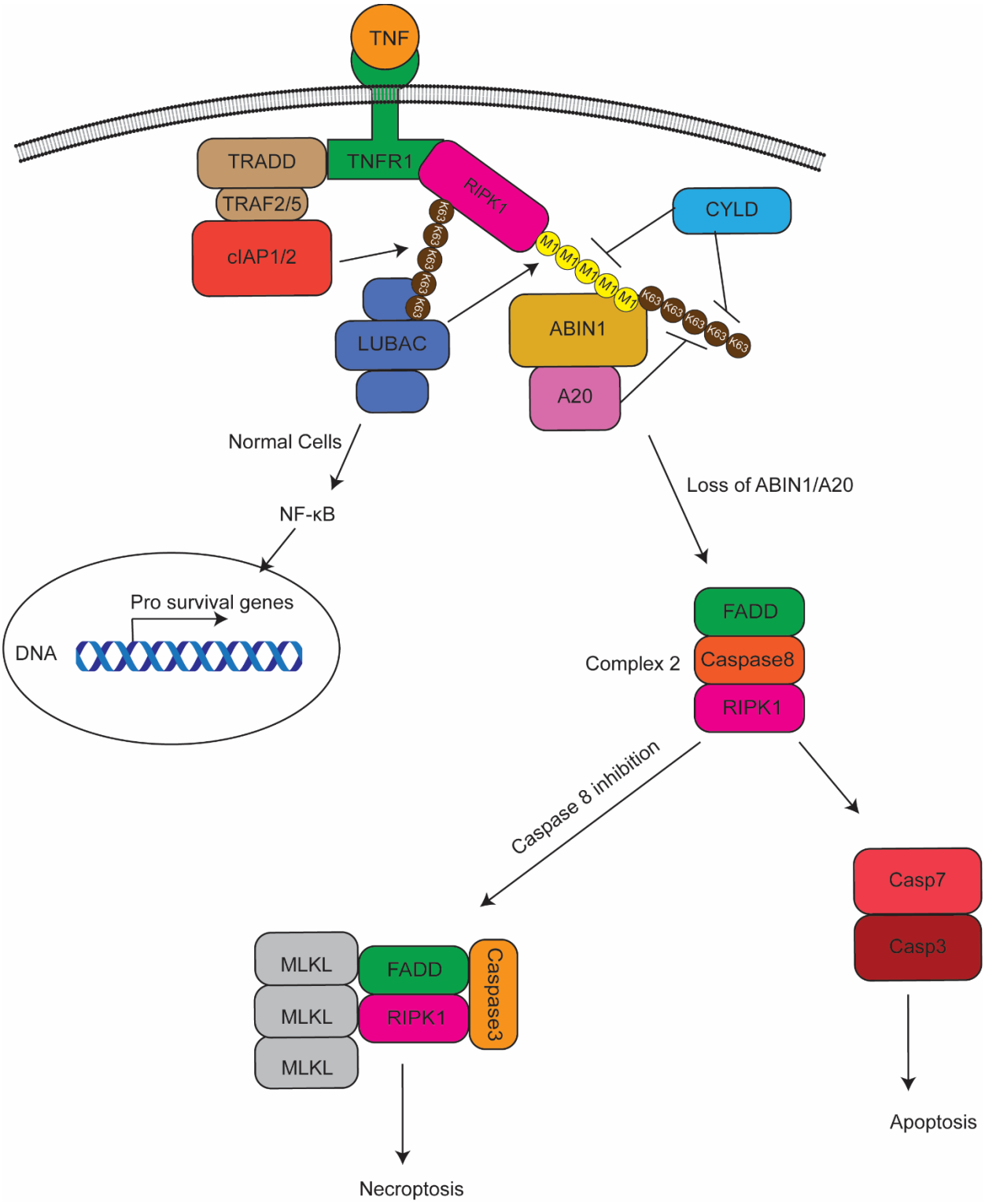
TNF
TRADD
TNFR1
RIPK1
TRAF2/5
cIAP1/2
CYLD
K63
M1
LUBAC
ABIN1
A20
Normal Cells
NF-κB
Pro survival genes
DNA
Loss of ABIN1/A20
FADD
Complex 2
Caspase8
RIPK1
Caspase 8 inhibition
Casp7
Casp3
MLKL
FADD
Caspase3
RIPK1
Apoptosis
Necroptosis

Figure 1.6

Upon TNF binding to TNFR1 Complex I consisting of TRADD, TRAF2/5, cIAP1/2, and RIPK1 is recruited. Subsequently the ubiquitin ligase LUBAC, which generates Met-1 ubiquitin chains, is recruited to Complex I. Generation of Met-1 ubiquitin chains on RIPK1 in turn recruits ABIN1 which provides a scaffolding for the ubiquitin editing enzyme A20. The ubiquitin modification by A20 prevents Complex II formation and upregulates NF-κB activation of pro survival genes. When ABIN1, A20 or LUBAC are disrupted Complex II forms, consisting of FADD, Caspase8, and RIPK1. Generation of Complex II leads to apoptosis by inducing Caspase7 and Caspase3 activation, or necroptosis when Caspase8 is inhibited and Caspase3 complexes with FADD and RIPK1 and recruits MLKL.

ABIN1: A negative regulator of NF-kB

ABIN1 is a binding partner of A20 that acts as a scaffolding protein to recruit A20 to the Tumor Necrosis Factor pathway and down regulate cell death[43]. A20 is a ubiquitin editing enzyme that prevents apoptosis and necrosis in response to TNF induced signaling. Upon the binding of TNF to TNF Receptor (TNFR), Complex I is formed, consisting of Tumor necrosis factor receptor type 1-associated DEATH domain protein (TRADD), TNFR Association Factor (TRAF) 2/5, cellular inhibitor of apoptosis protein1/2(cIAP1/2), LUBAC, and RIPK1[44]. RIPK1 in Complex I is then ubiquitinated with both Met-1 ubiquitin and Lys-63 ubiquitin by LUBAC and cIAP1/2 (Figure 1.6). A20 prevents the removal of Met-1 ubiquitin of RIPK1 by Ubiquitin carboxyl-terminal hydrolase (CYLD) and replacement of it with Lys-63 ubiquitin, preventing the formation of Complex II. When complex II is formed, consisting of RIPK1, FADD, and Caspase8, which can either induce apoptosis in a Caspase3 and Caspase7 dependent manner or necrosis by recruiting mixed lineage kinase domain-like (MLKL) to Complex II. In the absence of A20, Met-1 ubiquitin is removed from RIPK1 at an increased rate and Lys-63 ubiquitin can attach. Loss of the proteins responsible for modulating RIPK1 ubiquitination sensitizes cells to TNF induced cell death.

The role of ABIN1 is the recruitment of A20 to Complex I, when ABIN1 is absent cells become sensitized to cell death in a TNF dependent manner as if A20 was absent[45]. ABIN1 is recruited to the Met-1 ubiquitin chains on LUBAC or RIPK1 and then acting as a scaffolding protein for A20[46]. Loss of ABIN1's capacity to bind Met-1 ubiquitin causes it to become sensitized to TNF. The currently established role of ABIN1 is as a regulator of TNF dependent inflammation, dependent on its ability to bind Met-1 ubiquitin.

ABIN1 role in disease

The diseases most associated with ABIN1 are Lupus, Psoriasis, and autoimmune disorders[47-49]. The primary effect of ABIN1 mutations has been found to be related to changes in regulation of inflammatory signaling within cells. Lupus is characterized by B cells generating auto antibodies and an uncontrolled inflammatory response. Unregulated NF- kB activation occurs when TNF signaling is no longer being downregulated by ABIN1 upstream in the pathway. In Psoriasis it has been found that the TNF signaling is unregulated along with Interleukin-17, a pro inflammatory cytokine. Another factor is that normally ABIN1 recruits A20 to IKK for deubiquitinating activity[50]. In Psoriasis, instead of autoimmune signaling originating in B cells it instead comes from deregulated keratinocytes. Autoimmune disorders related to ABIN1 have been found to involve the two previous pathways as well as dysregulation of Toll Like Receptor(TLR)-Myeloid differentiation primary response 88 (MyD88)[49]. ABIN1 has been found to directly bind Interleukin-1 receptor-associated kinase 1 (IRAK1), dependent on its UBAN domain, and downregulate inflammatory signaling. Loss of regulation in these inflammatory pathways causes CD40 signaling activation and subsequent B cell activation with upregulated IκB

kinase (IKK) activation and c-Jun N-terminal kinase (JNK) signaling. While some of the exact signaling has been elucidated, there appear to be other increased inflammation unexplained by the current models.

Chapter 2: Results

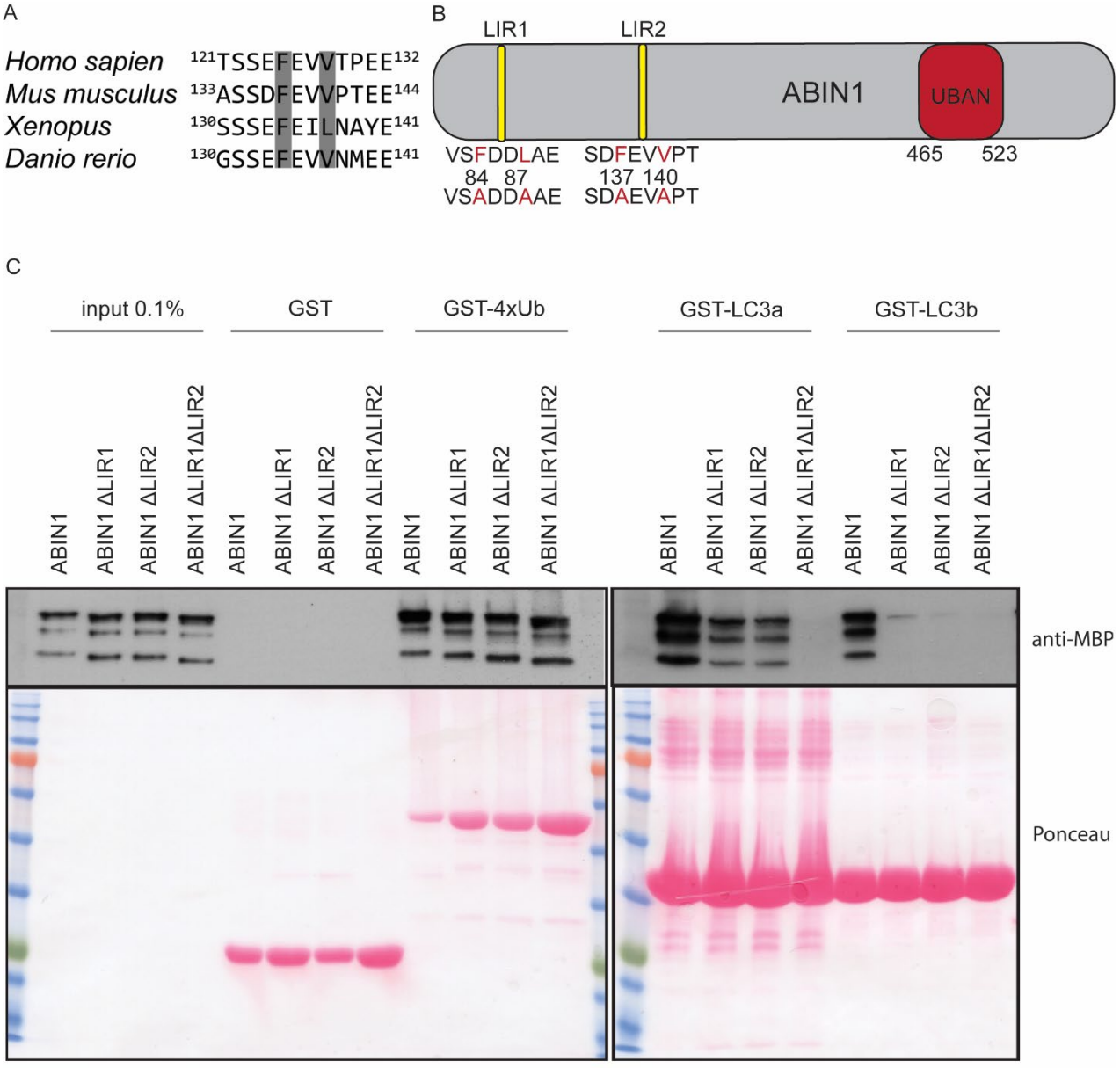

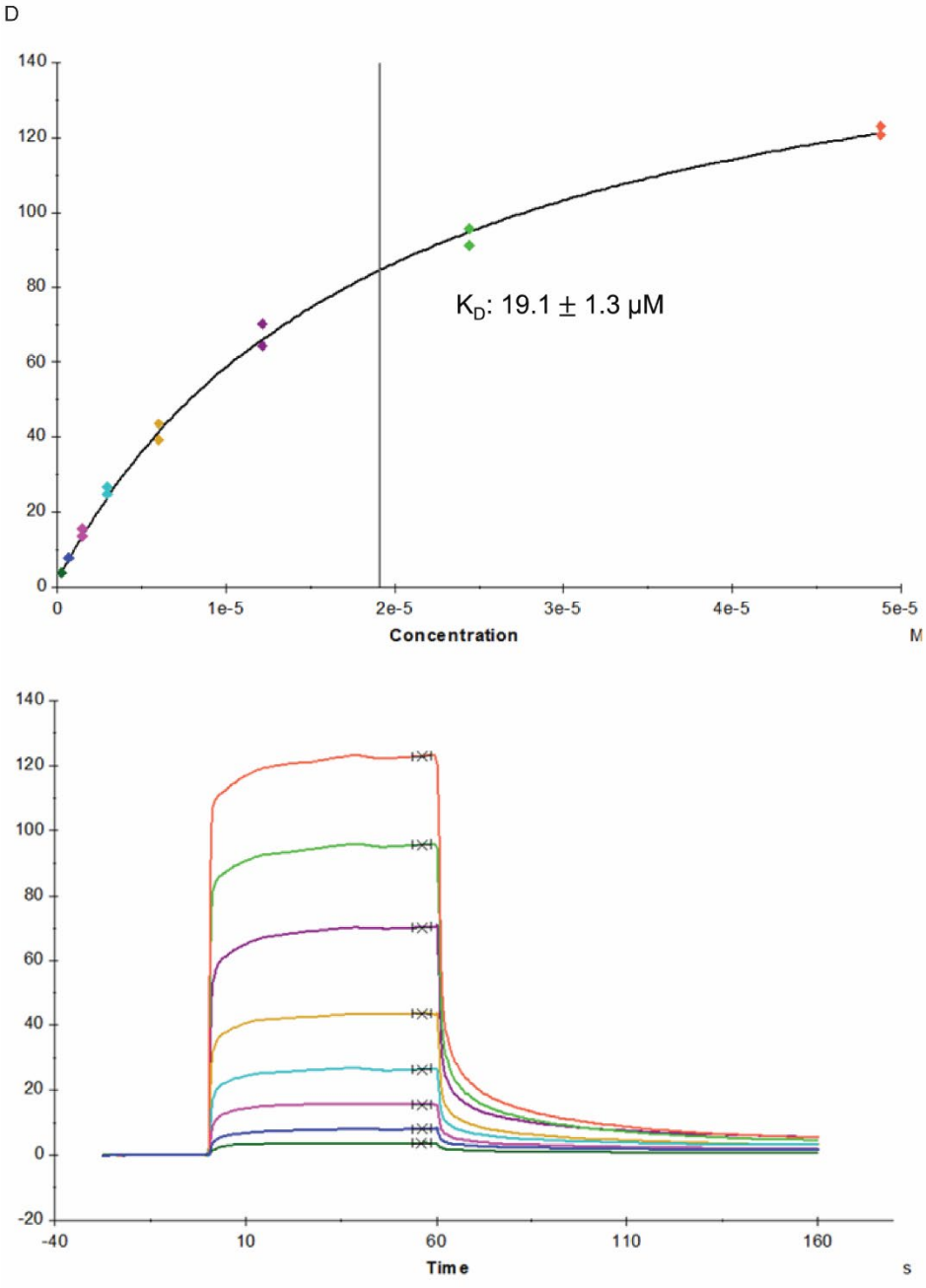

Figure 2.1

ABIN1 possesses the domains of an autophagy receptor and binds LC3

A) Evolutionarily conserved LIR domain of ABIN1 LIR motif. B) Schematic of ABIN1 mutations made to LIR domains to disrupt LC3 binding. C) GST pulldown using recombinant Ubiquitin, LC3a and LC3b with eluted MBP ABIN1. D) Surface Plasma Resonance using ABIN1 and bound LC3.

While searching for novel autophagy receptors ABIN1 was noted as a putative autophagy receptor due to its apparent LIR motifs discovered via bioinformatics using HHpred. Mutants were then generated by introducing two separate point mutations at the first LIR 1 F84A L87A, two separate point mutations at the second LIR 2 F137A V140A, or both LIRs mutated (LIR 1 LIR 2). A pull-down testing ABIN1's ability to bind LC3 dependent on these LIR domains was then performed, with 4xUbiquitin, which is generated using a plasmid with four ubiquitin expressed one after another so they will be expressed C-terminal Glycine to N-terminal Methionine the same way Met-1 ubiquitin are conjugated, which can used as a positive control as ABIN1 is known to bind linear ubiquitin chains. This pull-down showed that ABIN1 can directly bind both LC3a and LC3b, with increased binding to LC3a and showed that the binding is dependent on the LIR domains. While loss of only one LIR domain mildly disrupts their binding, mutations in both LIR domains completely disrupt ABIN1 LC3 interactions. We confirmed the binding affinity by performing surface plasmon resonance (SPR) using bound LC3 and flowing ABIN1 over that. From the data obtained from SPR we determined that ABIN1 has a dissociation constant (K_D) of 19.3±1.3μM.

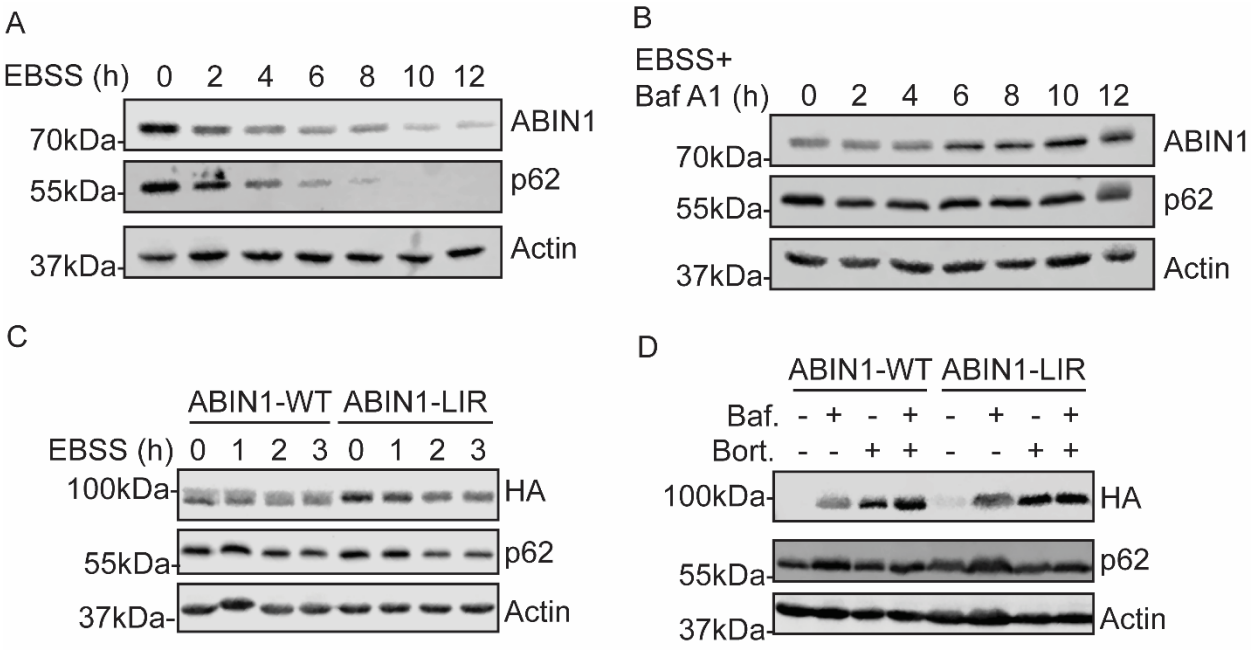

Figure 2.2

ABIN1 is degraded by the lysosomes upon inducing autophagy

Cells were lysed in RIPA buffer and run on SDS page for western blot analysis (representative of three individual experiments) A) HeLa cells were grown in EBSS for the indicated period. B) HeLa cells were grown in EBSS supplemented with 500nM Bafilomycin A1 for indicated period. C) HeLa cells stably expressing inducible recombinant ABIN tagged Strep-Strep-HA treated with Doxycycline for 16 hours and then cultured in EBSS for indicated time. D) HeLa cells stably expressing inducible recombinant ABIN tagged Strep-Strep-HA treated with Doxycycline for 16 hours and then treated with fresh media alone or supplemented with 500nM Bafilomycin A1, 100uM Bortezomib or both.

After establishing that ABIN1 can bind LC3 we looked at the effects of autophagy on endogenous ABIN1 levels. To examine ABIN1's response to autophagy induction we cultured HeLa cells in EBSS, a non-supplemented starvation medium known to induce autophagy due to nutrient deprivation and tracked the changes in ABIN1 levels over the time period along with p62, a known autophagy receptor. We observe that ABIN1 levels decrease upon autophagy induction that mirrors changes in p62. To confirm that EBSS was inducing autophagy we then blocked lysosomal degradation using Bafilomycin A1. When

HeLa cells were cultured in EBSS paired with Bafilomycin A1, to block lysosomal acidification, ABIN1 levels increase in parallel with p62. To examine the effects of mutating the LIR domain in ABIN1 levels in response to autophagy, we cloned WT ABIN1 and LIR1/2 ABIN1, hereafter referred to as ABIN1-WT and ABIN1-LIR, into pcDNA5/FRT/TO tagged with C terminal Strep-Strep-HA. We then stably expressed ABIN1-WT and ABIN1-LIR in HeLa TREX FRT cells. Expression of ABIN1-WT and ABIN1-LIR in HeLa cells was induced with doxycycline (dox) overnight, the next day media was replaced, and cells were cultured in EBSS for the indicated time. ABIN-WT and ABIN1-LIR levers were both found to be decreasing over the time course. To better understand the ways in which ABIN1 was being degraded, we utilized the Tet-Repressor system to induce the expression of ABIN1-WT and ABIN1-LIR with dox and then subsequently stopping the expression of ABIN1 by washing away the dox. As expression of ABIN1 was turned off, we prevented lysosomal degradation by treating with Bafilomycin A1, which prevent the acidification of lysosomes, prevented proteasomal degradation by treating with Bortezomib, which blocks the proteasome binding pocket, or treated with both drugs to prevent both forms of degradation. From this we determined that ABIN1 was degraded in both the proteasome and the lysosomes, and that the LIR mutant seemed to be resistant to it as it had no apparent difference between the bortezomib treated and bafilomycin/bortezomib treated samples. These findings show ABIN1 levels are decreasing upon autophagy induction and increasing upon inducing autophagy paired with blocking lysosomal degradation. These results show that ABIN1 is degraded in an autophagy-dependent manner and further support that ABIN1 is an autophagy receptor.

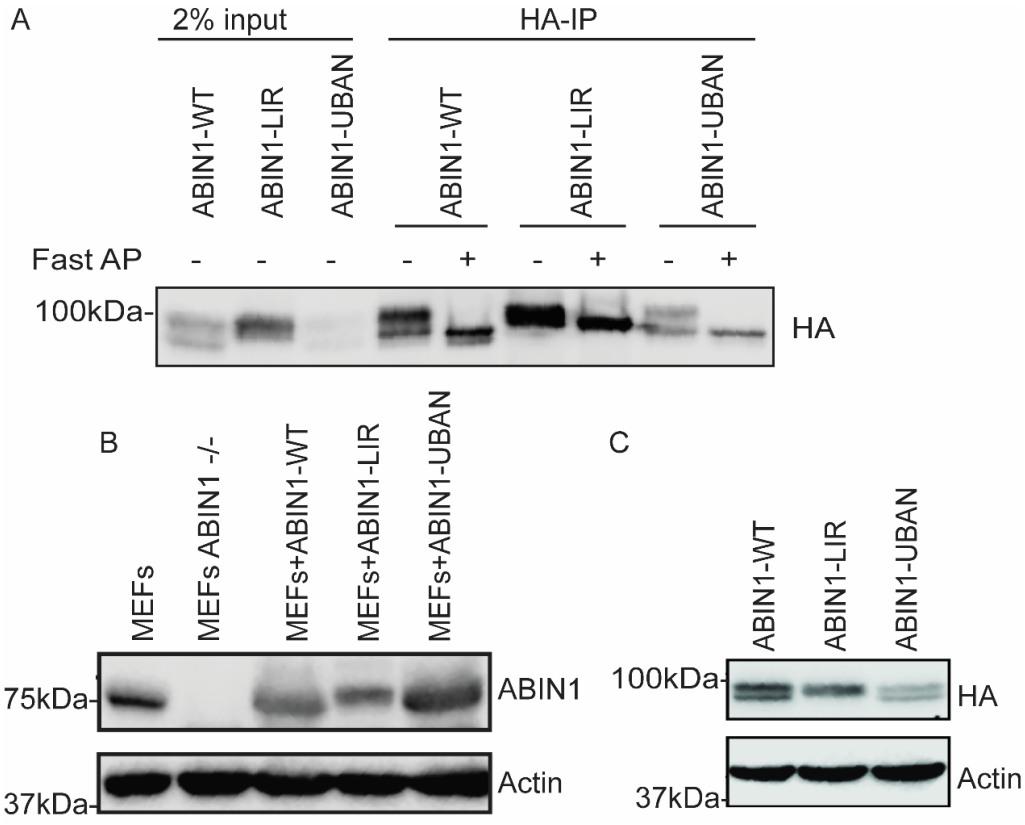

Figure 2.3

Mutations to the LIR domain of ABIN1 cause it to become hyperphosphorylated

A) Recombinant ABIN1 WT, LIR or UBAN tagged with Strep-Strep-HA transiently transfected in 293T cells. Immunoprecipitation with HA magnetic beads was done followed by treatment of the enriched protein with phosphatase. Samples were analyzed by western blot (representative of two individual experiments). Stable reconstituted ABIN1 cells lines untagged in ABIN1$^{-/-}$ MEFs (B) or Strep-Strep-HA tagged ABIN1 in HeLa TREX Cells.

Upon expressing ABIN1 WT and mutant LIR we noticed that mutations in the LIR domain caused ABIN1 to elicit a reduced electrophoretic mobility compared to ABIN1 WT. This reduced electrophoretic mobility is consistent during expression in HeLa, MEF, U2OS, and 293T cells. We looked to examine what post-translational modification was causing this and decided to examine the potential of phosphorylation. We expressed ABIN1-S-S-HA in 293T cells and then immune-precipitating ABIN1 using HA magnetic

beads and treating the enriched ABIN1 with phosphatase. This caused the ABIN1-WT, ABIN1-LIR and ABIN1-UBAN, which possess mutation at D485N F486N, to have increased electrophoretic mobility. This confirmed that ABIN1 is being phosphorylated and that upon loss of its LIR motif, causing loss of ability to bind LC3, ABIN becomes hyperphosphorylated.

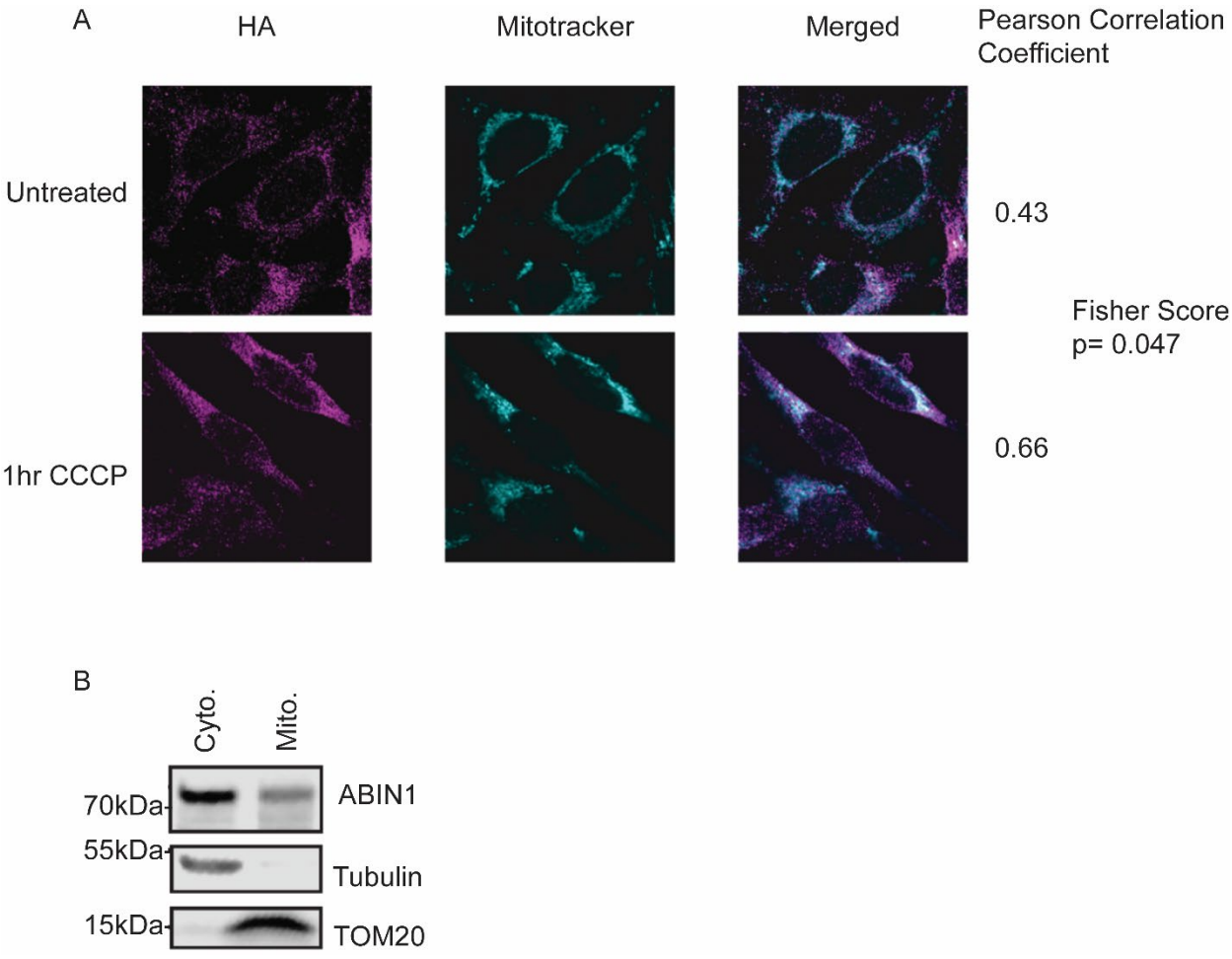

Figure 2.4

ABIN1 colocalizes with the mitochondria, this increases upon mitochondrial depolarization

A) HeLa TREX cells stably expressing ABIN1-S-S-HA were grown on coverslips overnight in the presence of 10ug/ml doxycycline. Cells were treated with 250nM MitoTracker Deep Red for 45 minutes before fixing with 4% formaldehyde and then immunofluorescence was done using anti-HA and colocalization of HA and MitoTracker was determined using Coloc 2 and Pearson Correlation was given, n>50. Fisher score was determined using Microsoft Excel. B) Thermofisher mitochondrial isolation kit was used on WT MEFs. Fractions were run on Bio Rad precast 4%-15% SDS page and analyzed by western blot (representative of three individual experiments).

After confirming that ABIN1 is degraded in an autophagy-dependent manner, we asked if ABIN1 co-localized with mitochondria. Towards this end, we examined ABIN1 in HeLa cells using Immunofluorescence (IF) by using MitoTracker to stain the mitochondria and then fixing with formaldehyde and immunostaining with HA antibody to detect HA-ABIN1. ABIN1 was found to colocalize with mitochondria and this colocalization increases upon treating cells with CCCP, a potent mitochondrial depolarizer. We further confirmed the interaction between ABIN1 and mitochondria by performing mitochondrial isolation and found that ABIN1 was in the mitochondrial fraction. We used tubulin as the control for the cytosolic fraction and TOM20 as the control for the mitochondrial fraction.

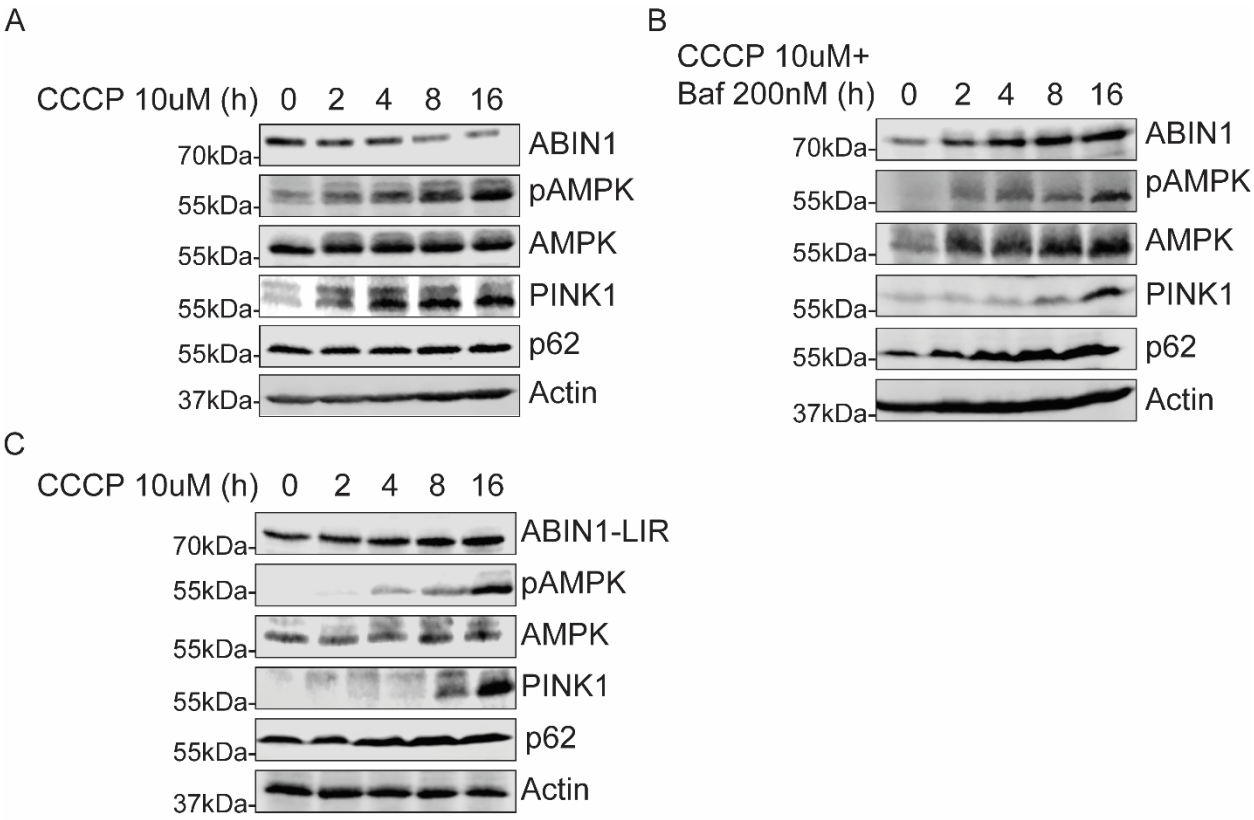

Figure 2.5

ABIN1 is degraded in a mitophagy specific manner dependent on its LIR domain

WT MEFs or MEFs reconstituted with LIR mutated ABIN1 were lysed in 1x Laemmli Buffer and run on Bio Rad TGX precast gels 4%-15% for western blot analysis (representative of three independent experiments) . A) MEFs treated with 10uM CCCP for the indicated period. B) MEFs were treated with 10uM CCCP and 200nM Bafilomycin A1 for the indicated period. C) ABIN1$^{-/-}$ MEFs were reconstituted with ABIN1-LIR and treated with 10uM CCCP for the indicated period.

To investigate the potential of ABIN1 as a mitophagy receptor, we selectively induced mitophagy using CCCP, a mitochondrial depolarizer, and examined changes in ABIN1. To monitor for mitophagy activation, we assessed the phosphorylation status of AMPK (pAMPK), which occurs during mitophagy induction due to increases in the ratio of AMP/ADP:ATP, and for the PINK1 levels, which is stabilized upon mitochondrial damage. We also assessed the levels of p62, which is not a primary mitophagy receptor but

is degraded during general autophagy. As expected, p62 levels did not decrease under these conditions, indicating that general autophagy wasn't induced. Actin was used as a loading control. In WT MEFs, ABIN1 levels decrease in as a result of mitochondrial depolarization, while pAMPK and PINK1 levels increase, thus indicating that mitophagy has been induced and suggesting that ABIN1 is degraded. In CCCP treated cells, p62 levels remained stable, indicating that general autophagy was not induced. However, when cells are treated with CCCP and Bafalomycin A1, ABIN1 levels increase despite the induction of mitophagy, as indicated from increases in PINK1 and pAMPK. We then looked at ABIN1 levels when ABIN1's ability to bind to LC3 is disrupted by inducing mitophagy in MEFs stably expressing ABIN1-LIR. Surprisingly, we found that ABIN1 levels increase with the treatment of CCCP. This shows that mitophagy-dependent degradation of ABIN1 is dependent on the LIR domain. Interestingly, we also observe that phosphorylation of AMPK appears to be decreased when the LIR domain of ABIN1 is mutated.

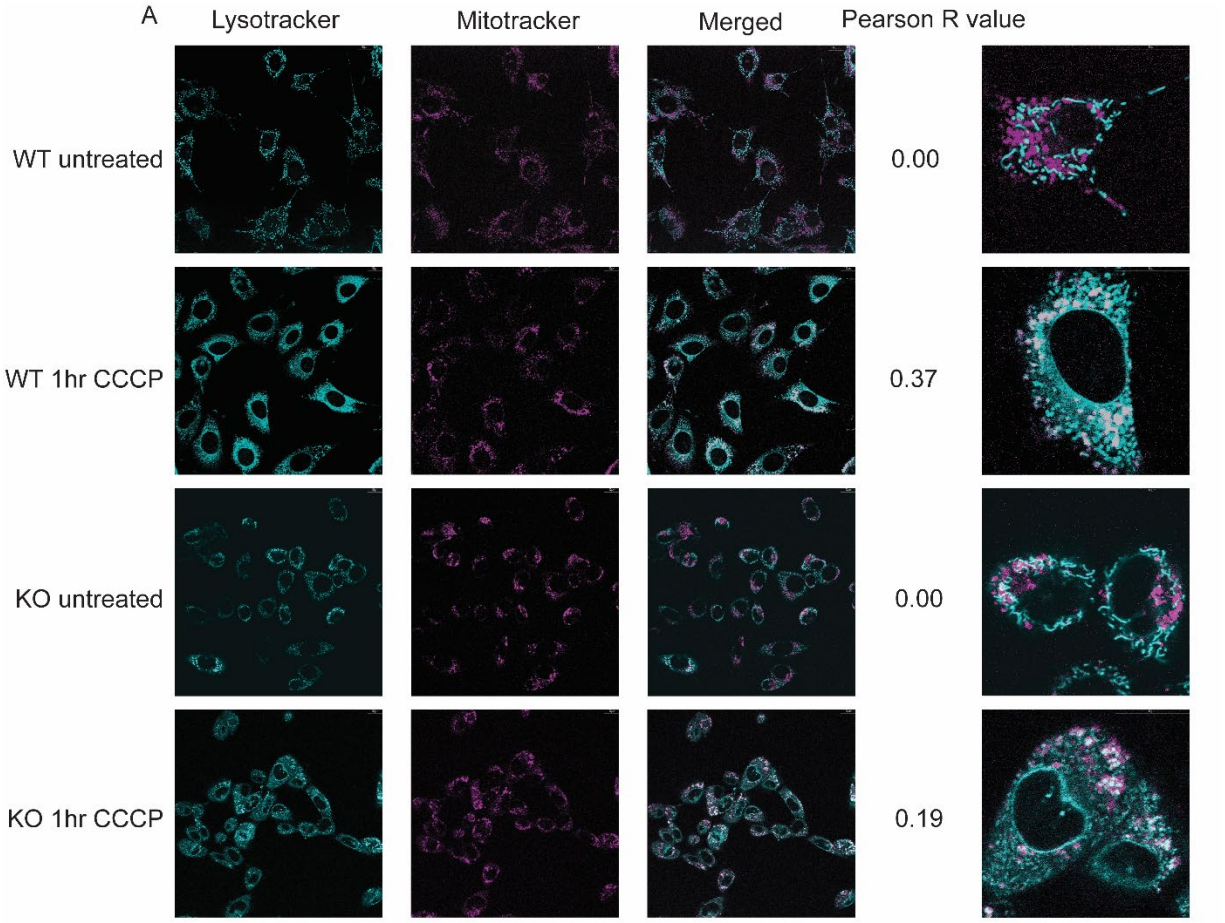

Fisher Value
WT untreated vs WT treated
p= 0.029
KO untreated vs KO treated
p= 0.047
WT treated vs KO treated
p= 0.068

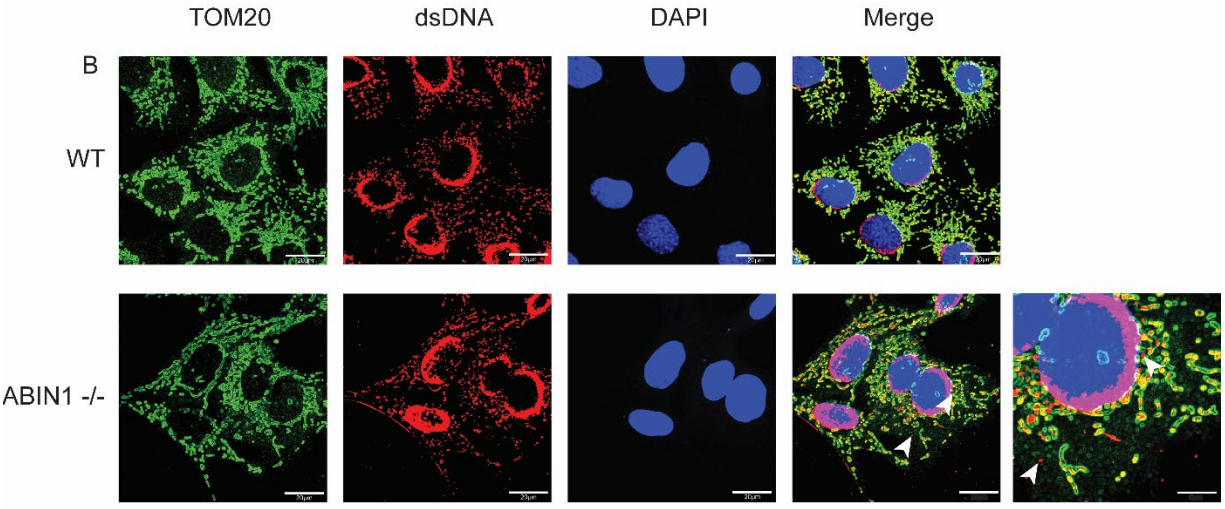

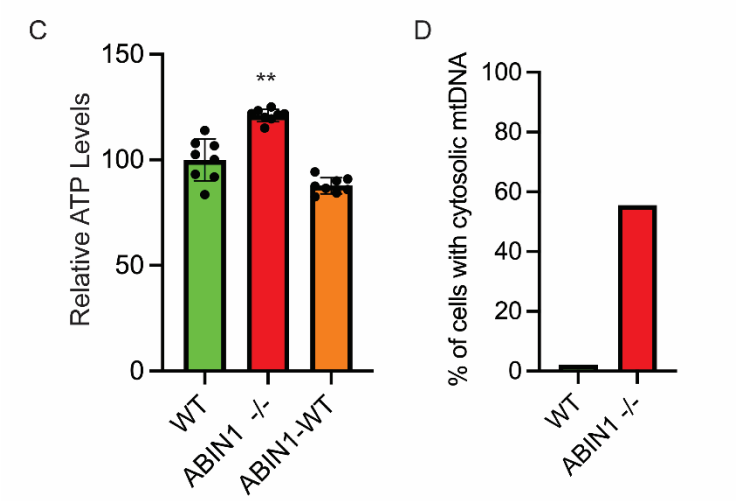

Figure 2.6

Loss of ABIN1 disrupts mitophagy and mitochondrial maintenance

A) WT MEFs or ABIN1$^{-/-}$ MEFs were grown on Labtech dishes and incubated with LysoTracker Blue DND-22 and MitoTracker Deep Red for 45 minutes and then imaged or for 30 minutes and then spiked with 10uM CCCP for an additional hour. Colocalization was determined using Coloc 2 in FIJI n>50. Fisher value was calculated using Microsoft excel. B) MEFs were grown on coverslips and then fixed with 4% formaldehyde before staining with TOM20 antibody, dsDNA antibody, and DAPI. C) Number of cells with 2 or more dsDNA puncta not overlapping with TOM20 was counted and graphed. D) ATP assay was used on MEFs WT, ABIN1$^{-/-}$, or reconstituted ABIN1 WT cells. Results were normalized to WT MEFs and analyzed by Student's t-test **p<0.01, n=8.

After establishing that ABIN1 colocalizes with the mitochondria, we examined if loss of ABIN1 affected mitochondrial maintenance in MEFs derived from ABIN1$^{-/-}$ mouse embryos. We examined if mitochondria would be sequestered to the autophagosomes at the same rate in ABIN1$^{-/-}$ MEFs as it was in WT MEFs. We incubated cells with MitoTracker and LysoTracker prior to damaging the mitochondria so that the organelles would be fluorescent before they were trafficked. We found that in both WT and ABIN1$^{-/-}$ cells untreated there was no colocalization of the mitochondria and lysosomes. Upon

treating with CCCP for 1 hour we found that there was no significant difference in WT MEFs compared to the ABIN1$^{-/-}$ MEFs, $p>0.05$. This showed that loss of ABIN1 had no major effect on the sequestering of mitochondria to autophagosomes. Mutations to ABIN1's UBAN domain causes Lupus like symptoms in mice, and the underlying cause is still unknown. Cytosolic mtDNA has separately been shown to cause Lupus like symptoms. Based on this we examined WT and ABIN1$^{-/-}$ cells for the presence of mtDNA in the cytosol, a phenomenon that does not usually occur in typical cells. We did this by immunostaining with a TOM20 antibody in combination with dsDNA antibody and then examining cells for the presence of dsDNA in the cytosol in places absent of accompanying TOM20 signal. Because the dsDNA antibody also stains nuclear DNA, DAPI was used to identify the nucleus and signal from the nucleus was not counted. For each cell type, 45 cells were scored for the presence of apparent mtDNA. We found that in ABIN1$^{-/-}$ cells ~50% of cells appeared to have dsDNA signal with no overlapping TOM20 signal while only ~3% of WT cells had the same phenomenon. This indicates that there is mtDNA in the cytosol of cells lacking ABIN1. We were also interested in assessing the abundance of mitochondria in ABIN1$^{-/-}$ cells compared to WT. To determine if there appeared to be more mitochondria in ABIN1$^{-/-}$ cells, ATP levels were quantified. We found that in cells lacking ABIN1 there were significantly higher ATP levels compared to WT cells, and that reconstituting WT ABIN1 in these cells reduced the ATP levels to those observed in WT cells.

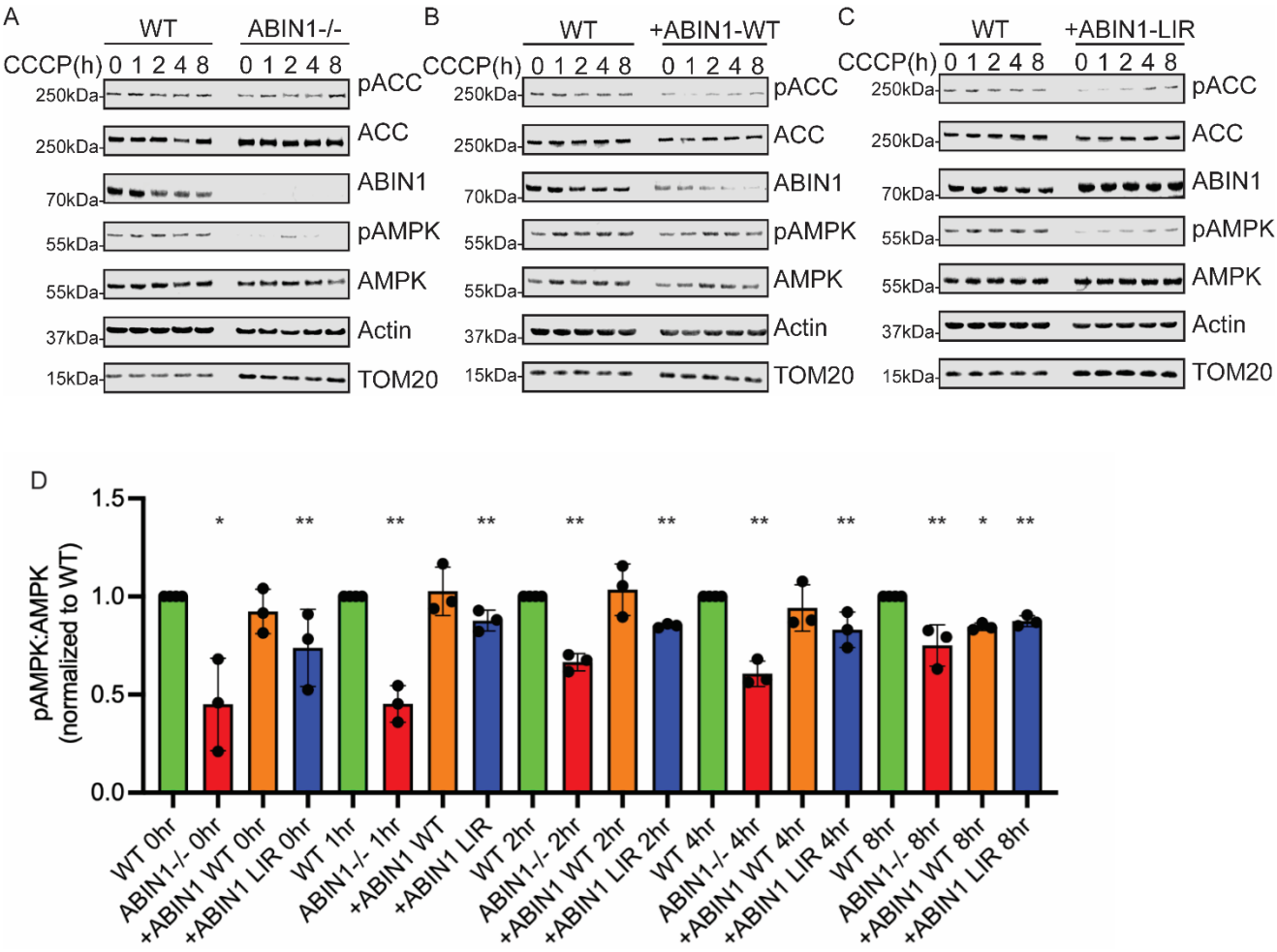

Figure 2.7

Loss of ABIN1 inhibits AMPK phosphorylation upon mitochondrial depolarization

A) WT MEFs as well as ABIN1$^{-/-}$ MEFs (A), reconstituted ABIN1-WT MEFs (B) or reconstituted ABIN1-LIR MEFs (C) were treated with CCCP for indicated time period and then analyzed by western blot (representative of 3 independent experiments). D) The ratio of pAMPK:AMPK levels for the ABIN1$^{-/-}$, +ABIN1-WT, or +ABIN1-LIR MEFs was normalized to the WT MEFs for each time point and compared using Student's t-test *$p<0.05$, **$p<0.01$.

Initial work to establish that ABIN1 is degraded in a mitophagy-dependent manner, a decrease in pAMPK was observed in ABIN1$^{-/-}$ cells expressing ABIN1-LIR following mitochondrial depolarization. To determine the domains in ABIN1 that are required for AMPK phosphorylation, we reconstituted ABIN1$^{-/-}$ cells with ABIN1-WT or ABIN1-LIR.

While reconstituting ABIN1$^{-/-}$ cells with ABIN1-WT restored the AMPK phosphorylation to levels found in WT MEFs, reconstituting cells with ABIN1-LIR mutants did not full restore the AMPK phosphorylation, suggesting that ABIN1-autophagasome interaction is required for AMPK phosphorylation upon mitochondrial depolarization.

Chapter 3: Discussion

The precise lysosomal degradation of cargo in response to autophagy activation requires autophagy adaptors and receptors. Of the UBAN domain containing proteins identified thus far as autophagy receptors, only NEMO and ABIN1 remained to be characterized as autophagy receptors. We found that ABIN1 binds directly to LC3 (Fig. 2.1 C,D) and is degraded in the lysosomes (Fig. 2.1 A,B) suggesting that it could function as an autophagy receptor. To further investigate this possibility, we used bioinformatics to identify putative LIR domains within ABIN1 that would facilitate a physical interaction with LC3. Mutational ablation of these two LIR motifs resulted in the inability for ABIN1 to interact with LC3 (Fig. 2.2 C).

Mitochondria regulation is a key process for maintaining cellular homeostasis. We provide evidence that cells lacking ABIN1 have a difference in their basal mitochondria level (Fig. 2.6 D). We first establish that ABIN1 is recruited to the mitochondria and this recruitment increases upon damage to the mitochondria (Fig. 2.4 A,B). After inducing mitophagy, we found that ABIN1 is degraded in a mitophagy specific manner (Fig. 2.5 A,B) and ABIN1's degradation is dependent on the LIR domains (Fig. 2.5 C). The changes in basal mitochondrial level are however not a result of any changes to mitochondrial fission or recruitment of mitochondria to autophagosomes (Fig. 2.6 A). Instead ABIN1 appears to be regulating mitophagy by regulating the phosphorylation of AMPK (Fig 2.7 A,B,D), dependent on ABIN1's LIR domain (Fig. 2,7 C,D). This suggests that ABIN1 may play a role in nutrient sensing of a cell.

Numerous western blot analysis indicates that ABIN1 displays a species with reduced electrophoretic mobility, reminiscent of phosphorylation. Utilizing an in vitro

phosphatase assay, we confirmed that ABIN1 is phosphorylated. Interestingly, we found that mutations in the LIR domains causes a quantitative ABIN1 hyperphosphorylation (Fig 2.3 A). At this time, we have not identified the kinase responsible for phosphorylating ABIN1 nor have we found the phosphatase responsible for dephosphorylating ABIN1. We hypothesize that dephosphorylation of ABIN1 either occurs after ABIN1 is recruited to the autophagosome or that the phosphorylation state of ABIN directs its localization within the cell.

Many genes have been linked to Lupus but the exact cause of this disease to date is still unknown. ABIN1 is one of the genes that has been correlated with Lupus in screenings and has been consistently found to be downregulated in these patients. Another point of interest is that mice with a mutation in the UBAN domain of ABIN1 have characteristic Lupus like symptoms, but the underlying mechanism for this phenotype remains unknown. Separately it has been found that mtDNA fragments in the cytoplasm cause lupus like symptoms. For these reasons we decided to examine cells lacking ABIN1 for the presence of mtDNA within the cytoplasm. Using immunofluorescence, we find that there is an increase in the amount of mtDNA present in the cytosol of cells lacking ABIN1 (Fig. 2.6 B). This suggests that ABIN1 senses depolarized mitochondrial and either directly or indirectly promotes mitophagy to maintain cellular homeostasis. Furthermore, in the absence of ABIN1, the detection of depolarized mitochondria is delayed leading to cytosol leakage of mtDNA which in turn elicits a strong inflammation response. Cytosolic mtDNA might elicit an inflammatory response by activating the cGAS-STING. These inflammatory pathways would in turn cause symptoms seen in Lupus patients as well as autoimmune disorder patients.

Materials and Methods

Antibodies and Reagents

Primary Antibodies were anti-ABIN1 (Proteintech 15104-1-AP 1:2000, Overnight 4°C), anti-p62 (Cell Signaling 5114 1:1000, overnight 4°C), anti-Actin (Sigma-Aldrich Mfcd00164531 1:5000, 1 hour room temperature), anti-HA.11(Biolegend 901513 1:5000, 1 hour room temperature), anti-AMPK(Cell Signaling 2532S 1:1000, overnight 4°C), anti-pAMPK(Cell Signaling 2535S 1:1000, overnight 4°C), anti-ACC(Cell signaling 3676T 1:1000, overnight 4°C), anti-pACC(11818T 1:1000, overnight 4°C), anti-PINK1(Novus BC100-494), anti-TOM20(Cell Signaling 42406S 1:1000, overnight 4°C). Secondary antibodies used were IRDye 800CW Goat anti-Rabbit (LI-COR 926-32211), IRDye 800CW Goat anti-Mouse (LI-COR 926-32210), IRDye 680RD Goat anti-Mouse (LI-COR 926-68070), Goat anti-Mouse IgG HRP (Invitrogen 31430), Goat anti-Rabbit IgG HRP (Santa Cruz Biotechnology sc-2357), Western Blotting Luminol Reagent (Santa Cruz Biotechnology sc-2048). Reagents used were Bafilomycin A1 (selleckchem s6494), CCCP (Cayman Chemical Company 11038), Bortezomib (Sigma Aldrich 5.04314), EBSS (HyClone SH30029.02), Doxycycline (Fisher BioReagents BP2653), Turbofect (Thermo Scientific R0531), 0.05% Trypsin-EDTA (Gibco 25300-054), DMEM 1X (Corning 10-013-CV), Penicillin-Streptomycin (HyClone SV30010), OPTI-MEM (Gibco 31985-062), PBS (Gibco 14190-144), FBS (Premium Select S11550H), DTT (Research Products International D11000), Protease Inhibitors (Roche 04693159001), PhosSTOP (Roche 04906845001), PMSF (Sigma Chemical Co. P-7626). Cell stains used were MitoTracker Deep Red FM(Thermo Fisher M22426), LysoTracker Blue DND-22(Thermo Fisher L7525).

Cell Lines

HeLa cells and HEK-293T cells were purchased from AtCc. Wild type and ABIN1$^{-/-}$ mouse embryonic fibroblasts were gifted to us by Dr. Averil Ma (UCSF). Cells were Cultured in DMEM with 4.5 g/L glucose, L-glutamine, and sodium pyruvate supplemented with 10% FBS and 100units/mL of Pen-Strep. Transfections were undertaken using 150µL of OPTI-MEM, 1ug of plasmid and 5ul of TurboFect. 16-24 hours after cells transfection reagent was applied media was changed. For flip-in cell lines, cells were transfected 900nG of pOG44and 100ng of plasmid containing FRT sequence and 16-24 hours later drug selection of choice was applied. For generation of retro virus HEK-293T cells were transfected with 1µg of pCG-Gag Pol and 2 µg pCG-VSVG, 1 µg transfer gene, and 5 µL TurboFect. Media was replaced on the plates 16-24 hours later and virus was then collected 48 hours later. Virus was applied to recipient cells for 16-24 hours, after which fresh media was given along with selection drug. Plasmids used include pRetroX-Tight-Puro, pcDNA5/FRT/TO-Hygro, and pIREShyg3.

Protein Purification

Recombinant MBP-ABIN1, GST, GST-LC3, and GST-4xUb was expressed in *E.coli* Rosetta and grown overnight at 37°C in LB supplemented with 100µg/ml ampicillin. Bacteria was then cultured until OD 0.600 before utilizing 0.5mM IPTG to induce expression. Cultures were incubated overnight at 37°C then pelleted and washed with 1xPBS. Pellets were frozen at -80°C for 1 hour. Pellets were resuspended in 500mM NaCl and PBS supplemented with 1mg/ml lysozymes, 1x Protease inhibitor, and 1mM DTT.

Pellets were sonicated until lysate was no longer viscous. Cellular debris were pelleted and supernatant was incubated with Glutathione Sepharose beads for GST purification or Amylose resin beads for MBP purification. Beads and supernatant were incubated for 3 hours at 4°C. Beads were washed 4x with 500mM NaCl and PBS before resuspending in PBS. MBP-ABIN1 was eluted using 100mM Maltose.

Pull Downs

Pull downs were performed using purified GST, GST-4xUB, GST-LC3a, and GST-LC3b bound to Glutathione beads along with eluted MBP-ABIN1 to determine binding. ABIN1 was incubated with GST, GST 4xUb, GST-LC3a, or GST-LC3b in 1x PBS for 1 hour. Beads were spun down and washed 3x with PBS before running on SDS page and analyzing by western blot.

Degradation Assay

HeLa cells stably expressing a Dox inducible ABIN1 were treated with 10nM Dox for 16 hours and then washed with PBS and given fresh media. When the fresh media was applied cells were treated with bortezomib, Bafilomycin A1, or a combination of both, to determine the modes of degradation of ABIN1.

Autophagy Assay

To examine the response of ABIN1 to general autophagy, wild type HeLa cells were cultured in DMEM supplemented with 10% FBS and Pen-Strep until approximately 80% confluent. Cells were then then washed with PBS and cultured in EBSS with or without 500nM Bafilomycin A1. Cells were harvested by scraping and then lysed in ice cold RIPA

buffer supplemented with protease inhibitors and DTT. Extract was combined with Laemmli sample buffer and run on an SDS page for Western blotting.

Mitophagy Assay

To examine the response of ABIN1 to mitophagy, WT and ABIN1-LIR MEFs were cultured in DMEM supplemented with 10% FBS and Pen-Strep until approximately 80% confluent. Cells were then washed with PBS then cultured in FBS free media for one hour. Fresh media supplemented with 10% FBS and Pen-strep was then applied along with 10μM CCCP alone or in combination with 200nM Bafilomycin A1. Cells were harvested by scraping and then lysed in RIPA buffer supplemented with protease inhibitors and DTT. Lysates were combined with 4x Laemmli sample buffer and run on an SDS page for Western blotting.

ABIN1-HA IP and Dephosphorylation Assay

293T cells were transiently transfected using turbofect with ABIN1-Strep-Strep-HA WT, LIR mutant, or UBAN mutant and grown for ~36 hours on 10cm dishes. Cells were collected by trypsinization and washed with 1xPBS. Cells were then resuspended in 500mL of 50mM Tris-HCl, 150mM NaCl, 0.1%NP-40, 10% glycerol, 1x Protease Inhibitor cocktail, 1mM PMSF, and 10mM NEM. These tubes were then incubated on ice for 20 minutes, sonicated 5 seconds on 5 seconds off for 1 minute on ice, and then clarified by centrifugation 15,000 rpm, 20 minutes, 4°C. Supernatants were transferred to fresh tubes and 10μl was saved for input. The remaining supernatant was incubated with magnetic HA beads (Thermo Scientific 88836) for 3 hours on a rotating wheel at 4°C. Afterwards beads were washed with 500μL of the lysis buffer minus glycerol five times. Beads were then

resuspended in 32µL of 20mM Tris-HCl pH 7.5, 150mM NaCl, 0.2% Triton X-100 and 1x Protease Inhibitor cocktail. This was then split evenly into two fresh tubes. These fresh tubes then received 2ul of 0.5M Tris-HCl pH 8, 1M NaCl, 100mM MgCl, and 10mM DTT. One tube then received 2uL of FastAP Thermosensitive Alkaline Phosphatase (Thermo Scientific EF0651) and the other tube received 2µL of resuspension buffer. The tubes were all incubated at 37°C for 1 hour. Each tube was then given 5µL of Laemmli buffer before running on a 10% agarose SDS page and subsequently analyzed by Western blot.

AMPK phosphorylation assay

Cells were cultured in DMEM supplemented with 10% FBS and Pen-Strep until ~80% confluent. Cells were washed once with prewarmed serum free DMEM and then serum starved for 1 hour in serum free DMEM. Media was changed to DMEM supplemented with 10% FBS and treated with 10uM CCCP for various time periods. Cells were collected by scraping and then lysed in 25mM Tris-HCl pH 7.5, 150mM NaCl, 0.2% NP-40, 1x protease inhibitor, 1x PhosSTOP and 1mM PMSF. Protein concentration was calculated using Thermo Scientific Pierce BCA Protein Assay Kit (23227). Samples were combined with Invitrogen 4x NuPAGE Sample buffer (NP0007) and 1mM DTT and incubated at 70° for 10 minutes. 20ug of each sample was run on a NuPAGE Bis-Tris 4-12% gel (NP0323BOX) and subsequently transferred for western blot analysis.

Immunofluorescence/Fixed Cells

For fixed cell images HeLa or MEF cells were grown overnight on cover slips, in the presence of 1ug/ml Dox for HeLa cells. The next day, dishes were washed with PBS and then cells were fixed with 4% formaldehyde in 1x PBS for 15 minutes at room temperature.

Cells were then washed 3x with 0.2% Triton X-100 in 1xPBS for 5 minutes each. Coverslips were transferred to a humidity chamber and blocked with 2% BSA, 1xTBS, 0.1% Tween-20 for 1 hour. Blocking reagent was removed and primary antibody was applied at 1:200 in blocking solution for 1 hour. Coverslips were then washed 3x with 1xTBS 0.1% Tween-20 for 5 minutes each. Secondary antibody was then applied at 1:200 in 5% BSA 1xTBS 0.1% Tween-20 for 1 hour. Coverslips were then washed 3x with 1xTBS 0.1% Tween 20 with the 3rd and final wash being supplemented with .1μg/ml DAPI. Coverslips were then mounted to a slide using mowiol and allowed to dry overnight before imaging.

Immunofluorescence/Live Cell imaging

For live cell imaging, MEFs were seeded onto glass bottom LabTek dishes with a microwell. For live cell imaging of mitochondria, cells were given fresh media prior to treating with 250nM Mitotracker Deep Red FM in prewarmed media for 45 minutes. For live cell imaging of lysosomes, cells were given fresh media prior to treating with 75nM Lysotracker Blue DND-22 for 1 hour. For examining colocalization of mitochondria and lysosomes, MEFS were treated with both Mitotracker and Lysotracker for 30 minutes before CCCP was added to the cells for 1 hour. Prior to imaging Mitotracker or Lysotracker were washed off with 1xPBS and cells were given CO2 independent media supplemented with 10% FBS.

Statistical Analysis

Western blots were analyzed after incubation with antibodies using a LI-COR Odyssey XF and intensity of bands was quantified using Empiria Studio 2.3. Colocalization was calculated using the Coloc 2 plugin in Fiji and Pearson Correlation coefficient was used.

LITERATURE CITED

1. Grumati, P. and I. Dikic, *Ubiquitin signaling and autophagy.* J Biol Chem, 2018. **293**(15): p. 5404-5413.
2. Schaaf, M.B., et al., *Autophagy in endothelial cells and tumor angiogenesis.* Cell Death Differ, 2019. **26**(4): p. 665-679.
3. Cherepanova, N., S. Shrimal, and R. Gilmore, *N-linked glycosylation and homeostasis of the endoplasmic reticulum.* Curr Opin Cell Biol, 2016. **41**: p. 57-65.
4. Kim, J., et al., *AMPK and mTOR regulate autophagy through direct phosphorylation of Ulk1.* Nat Cell Biol, 2011. **13**(2): p. 132-41.
5. Pyo, J.O., J. Nah, and Y.K. Jung, *Molecules and their functions in autophagy.* Exp Mol Med, 2012. **44**(2): p. 73-80.
6. Kim, J. and K.L. Guan, *mTOR as a central hub of nutrient signalling and cell growth.* Nat Cell Biol, 2019. **21**(1): p. 63-71.
7. Cheong, H., et al., *The Atg1 kinase complex is involved in the regulation of protein recruitment to initiate sequestering vesicle formation for nonspecific autophagy in Saccharomyces cerevisiae.* Mol Biol Cell, 2008. **19**(2): p. 668-81.
8. Itakura, E. and N. Mizushima, *Characterization of autophagosome formation site by a hierarchical analysis of mammalian Atg proteins.* Autophagy, 2010. **6**(6): p. 764-76.
9. Nakatogawa, H., *Mechanisms governing autophagosome biogenesis.* Nat Rev Mol Cell Biol, 2020. **21**(8): p. 439-458.
10. Gomez-Sanchez, R., S.A. Tooze, and F. Reggiori, *Membrane supply and remodeling during autophagosome biogenesis.* Curr Opin Cell Biol, 2021. **71**: p. 112-119.
11. Hamasaki, M., et al., *Autophagosomes form at ER-mitochondria contact sites.* Nature, 2013. **495**(7441): p. 389-93.
12. Itakura, E., et al., *Beclin 1 forms two distinct phosphatidylinositol 3-kinase complexes with mammalian Atg14 and UVRAG.* Mol Biol Cell, 2008. **19**(12): p. 5360-72.
13. Kuma, A., et al., *Formation of the approximately 350-kDa Apg12-Apg5.Apg16 multimeric complex, mediated by Apg16 oligomerization, is essential for autophagy in yeast.* J Biol Chem, 2002. **277**(21): p. 18619-25.
14. Burman, C. and N.T. Ktistakis, *Autophagosome formation in mammalian cells.* Semin Immunopathol, 2010. **32**(4): p. 397-413.
15. Garcia, D. and R.J. Shaw, *AMPK: Mechanisms of Cellular Energy Sensing and Restoration of Metabolic Balance.* Mol Cell, 2017. **66**(6): p. 789-800.
16. Shackelford, D.B. and R.J. Shaw, *The LKB1-AMPK pathway: metabolism and growth control in tumour suppression.* Nat Rev Cancer, 2009. **9**(8): p. 563-75.
17. Carling, D., V.A. Zammit, and D.G. Hardie, *A common bicyclic protein kinase cascade inactivates the regulatory enzymes of fatty acid and cholesterol biosynthesis.* FEBS Lett, 1987. **223**(2): p. 217-22.
18. Laplante, M. and D.M. Sabatini, *mTOR signaling in growth control and disease.* Cell, 2012. **149**(2): p. 274-93.
19. Johansen, T. and T. Lamark, *Selective Autophagy: ATG8 Family Proteins, LIR Motifs and Cargo Receptors.* J Mol Biol, 2020. **432**(1): p. 80-103.

20. Pankiv, S., et al., *p62/SQSTM1 binds directly to Atg8/LC3 to facilitate degradation of ubiquitinated protein aggregates by autophagy.* J Biol Chem, 2007. **282**(33): p. 24131-45.
21. Khaminets, A., C. Behl, and I. Dikic, *Ubiquitin-Dependent And Independent Signals In Selective Autophagy.* Trends Cell Biol, 2016. **26**(1): p. 6-16.
22. Hershko, A. and A. Ciechanover, *THE UBIQUITIN SYSTEM.* Annual Review of Biochemistry, 1998. **67**(1): p. 425-479.
23. French, M.E., C.F. Koehler, and T. Hunter, *Emerging functions of branched ubiquitin chains.* Cell Discov, 2021. **7**(1): p. 6.
24. Collins, G.A. and A.L. Goldberg, *The Logic of the 26S Proteasome.* Cell, 2017. **169**(5): p. 792-806.
25. Olzmann, J.A., et al., *Parkin-mediated K63-linked polyubiquitination targets misfolded DJ-1 to aggresomes via binding to HDAC6.* J Cell Biol, 2007. **178**(6): p. 1025-38.
26. Lazarou, M., et al., *The ubiquitin kinase PINK1 recruits autophagy receptors to induce mitophagy.* Nature, 2015. **524**(7565): p. 309-314.
27. Khaminets, A., et al., *Regulation of endoplasmic reticulum turnover by selective autophagy.* Nature, 2015. **522**(7556): p. 354-8.
28. Zheng, Y.T., et al., *The adaptor protein p62/SQSTM1 targets invading bacteria to the autophagy pathway.* J Immunol, 2009. **183**(9): p. 5909-16.
29. Mandell, M.A., et al., *TRIM proteins regulate autophagy: TRIM5 is a selective autophagy receptor mediating HIV-1 restriction.* Autophagy, 2014. **10**(12): p. 2387-8.
30. Baechler, B.L., D. Bloemberg, and J. Quadrilatero, *Mitophagy regulates mitochondrial network signaling, oxidative stress, and apoptosis during myoblast differentiation.* Autophagy, 2019. **15**(9): p. 1606-1619.
31. Pickles, S., P. Vigie, and R.J. Youle, *Mitophagy and Quality Control Mechanisms in Mitochondrial Maintenance.* Curr Biol, 2018. **28**(4): p. R170-R185.
32. Narendra, D., et al., *Parkin is recruited selectively to impaired mitochondria and promotes their autophagy.* J Cell Biol, 2008. **183**(5): p. 795-803.
33. Narendra, D.P., et al., *PINK1 is selectively stabilized on impaired mitochondria to activate Parkin.* PLoS Biol, 2010. **8**(1): p. e1000298.
34. Thurston, T.L., et al., *The TBK1 adaptor and autophagy receptor NDP52 restricts the proliferation of ubiquitin-coated bacteria.* Nat Immunol, 2009. **10**(11): p. 1215-21.
35. Otten, E.G., et al., *Ubiquitylation of lipopolysaccharide by RNF213 during bacterial infection.* Nature, 2021. **594**(7861): p. 111-116.
36. Miyashita, H., et al., *Crosstalk Between NDP52 and LUBAC in Innate Immune Responses, Cell Death, and Xenophagy.* Front Immunol, 2021. **12**: p. 635475.
37. Hernandez, D., et al., *Interferon-Inducible E3 Ligase RNF213 Facilitates Host-Protective Linear and K63-Linked Ubiquitylation of Toxoplasma gondii Parasitophorous Vacuoles.* mBio, 2022. **13**(5): p. e0188822.
38. Xu, Y., et al., *A Bacterial Effector Reveals the V-ATPase-ATG16L1 Axis that Initiates Xenophagy.* Cell, 2019. **178**(3): p. 552-566 e20.
39. Singh, A., S.L. Kendall, and M. Campanella, *Common Traits Spark the Mitophagy/Xenophagy Interplay.* Front Physiol, 2018. **9**: p. 1172.

40. West, A.P. and G.S. Shadel, *Mitochondrial DNA in innate immune responses and inflammatory pathology.* Nat Rev Immunol, 2017. **17**(6): p. 363-375.
41. Akira, S., S. Uematsu, and O. Takeuchi, *Pathogen recognition and innate immunity.* Cell, 2006. **124**(4): p. 783-801.
42. Kim, J., et al., *VDAC oligomers form mitochondrial pores to release mtDNA fragments and promote lupus-like disease.* Science, 2019. **366**(6472): p. 1531-1536.
43. Klinkenberg, M., et al., *Functional redundancy of the zinc fingers of A20 for inhibition of NF-kappaB activation and protein-protein interactions.* FEBS Lett, 2001. **498**(1): p. 93-7.
44. Priem, D., G. van Loo, and M.J.M. Bertrand, *A20 and Cell Death-driven Inflammation.* Trends Immunol, 2020. **41**(5): p. 421-435.
45. Kattah, M.G., et al., *A20 and ABIN-1 synergistically preserve intestinal epithelial cell survival.* J Exp Med, 2018. **215**(7): p. 1839-1852.
46. Dziedzic, S.A., et al., *ABIN-1 regulates RIPK1 activation by linking Met1 ubiquitylation with Lys63 deubiquitylation in TNF-RSC.* Nat Cell Biol, 2018. **20**(1): p. 58-68.
47. Harirchian, P., et al., *A20 and ABIN1 Suppression of a Keratinocyte Inflammatory Program with a Shared Single-Cell Expression Signature in Diverse Human Rashes.* J Invest Dermatol, 2019. **139**(6): p. 1264-1273.
48. Brady, M.P., et al., *TNIP1/ABIN1 and lupus nephritis: review.* Lupus Sci Med, 2020. **7**(1).
49. Nanda, S.K., et al., *Polyubiquitin binding to ABIN1 is required to prevent autoimmunity.* J Exp Med, 2011. **208**(6): p. 1215-28.
50. Catrysse, L., et al., *A20 in inflammation and autoimmunity.* Trends Immunol, 2014. **35**(1): p. 22-31.